

PROPERTIES OF U₃O₈-ALUMINUM CERMET FUEL (U)

OCTOBER 1989

Patent Status

This internal management report is being transmitted without DOE patent clearance, and no further dissemination or publication shall be made of the report without prior approval of the DOE-SR patent counsel.

Handwritten notes:
JFH
2/16/90

Handwritten notes:
2/16/90
J. K. ...
...

Westinghouse Savannah River Company
Savannah River Site
Aiken, SC 29808



PREPARED FOR THE U.S. DEPARTMENT OF ENERGY UNDER CONTRACT DE-AC09-88SR18035



WSRC-RP-89-981

PROPERTIES OF U₃O₈-ALUMINUM CERMET FUEL

AUTHOR

H. B. Peacock

Approved by:

**J. M. Stone
Manager, Materials Technology**

OCTOBER 1989

**Westinghouse Savannah River Company
Savannah River Site
Aiken, SC 29808**

ABSTRACT

Nuclear fuel elements containing U_3O_8 dispersed in an aluminum matrix have been used in research and test reactors for about 30 years. These elements, sometimes called cermet fuel, are made by powder metallurgical methods (PM) and can accommodate up to approximately 50 wt % uranium in the core section of extruded tubes.

Cermet fuel elements have been fabricated and irradiated at the Savannah River Site (SRS). Irradiation behavior is excellent. Extruded tubes with up to 50 wt % uranium have been successfully irradiated to fission densities of about 2×10^{21} fissions per cc of core.

Physical, mechanical, and chemical properties of cermet fuels are assembled into a reference document. Results will be used by Argonne National Laboratory to design cermet fuel elements for possible use in the New Production Reactor at SRS.

CONTENTS

	PAGE
1.0 U ₃ O ₈ -Aluminum Fuel.....	1
1.1 Introduction.....	1
1.2 Background of U ₃ O ₈ -Aluminum Dispersion Fuels.....	1
2.0 Physical and Mechanical Properties.....	2
2.1 Composition	3
2.1.1 Powder Preparation.....	3
2.1.2 Grinding.....	6
2.1.3 Blending.....	6
2.1.4 Compaction	6
2.1.5 Coextrusion.....	6
2.1.6 Rolling.....	10
2.2 Density.....	10
2.2.1 Powders.....	10
2.2.2 Extruded Tubes.....	12
2.3 Thermodynamic Properties.....	16
2.3.1 Specific Heat.....	16
2.4 Thermal Conductivity.....	16
2.4.1 Uranium Octaoxide (U ₃ O ₈).....	20
2.4.2 U ₃ O ₈ -Aluminum Mixtures.....	20
2.5 Linear Expansion.....	24
2.6 Mechanical Properties.....	26
2.6.1 Unirradiated.....	26
2.6.1.1 Tensile and Elongation	26
2.6.1.2 Bond Strength	26
2.6.2 High Temperature Strength	29
2.6.3 Irradiated	29
3.0 Chemical Properties.....	29
3.1 Low Temperature Reactions	32
3.1.1 Reaction Products.....	32
3.2 Exothermic Reactions.....	36

CONTENTS (Continued)

	PAGE
4.0 Irradiation Performance	45
4.1 Irradiation Conditions.....	45
4.2 Microstructure	45
4.3 Swelling and Blister Threshold Temperature	49
4.3.1 Swelling.....	49
4.3.2 Blistering.....	52
5.0 In-Reactor Fuel Behavior	57
5.1 Fuel Element Failures.....	57
5.2 Severe Accident Tests.....	57
6.0 Fission Product Release.....	59
7.0 Fabriciability.....	60
8.0 Reprocessibility	60
8.1 Unirradiated Fuel.....	60
8.2 Irradiated Fuel	64
9.0 References	65

LIST OF FIGURES

	PAGE
1 Powder Metallurgy Process at SRS.....	4
2 Typical Photomicrographs for U ₃ O ₈ Produced by Calcining UO ₃ at 800°C in a Low Grade Nitrogen/Air Atmosphere.....	5
3 Test of Modified Tumbling Mixer.....	8
4 Longitudinal and Transverse Sections From an Extruded U ₃ O ₈ -Al Fuel Tube Containing 80 wt % and 59 wt % oxide.....	9
5 Void Content For Extruded Reactor Fuel Tubes Containing U ₃ O ₈ and Aluminum.....	13
6 Aluminum and Uranium Oxide Volume Fractions and Tube Loadings for Extruded PM Fuel Tubes	15
7 Specific Heat of Aluminum and Triuranium Octaoxide (U ₃ O ₈).....	19
8 Thermal Conductivities of Non-stoichiometric Uranium Oxides Relative to that for Stoichiometric UO ₂	21
9 Effect of Temperature on the Thermal Conductivity of U ₃ O ₈	22
10 Calculated Thermal Conductivity Ratio (k_m/k_{Al}) for U ₃ O ₈ /Aluminum Mixtures.....	23
11 Relative Thermal Expansion of UO _{2.63} and UO _{2.67}	25
12 Strength and Elongation at 25°C for Extruded U ₃ O ₈ -Al Fuel Tubes.....	27
13 Bond Strength for Coextruded Tubes and Rolled Fuel Plates.....	28
14 Load - Extension Data for Unirradiated, Irradiated, and Annealed 8001 Aluminum Alloy.....	31
15 Thermal Reaction in SRS Extruded and Unirradiated U ₃ O ₈ -Al Cermet Tube Sections.....	33
16 Conversion of U ₃ O ₈ to U ₄ O ₉ in Heated U ₃ O ₈ -Al PM Compacts at Different Temperatures	34
17 Conversion of U ₃ O ₈ to U ₄ O ₉ in U ₃ O ₈ -Al PM Compacts With Time at Constant Temperature and Pressure.....	35
18 Effect of Pressure on U ₃ O ₈ to U ₄ O ₉ Conversion Reaction.....	37

LIST OF FIGURES (Continued)

	PAGE
19 Energy Release as a Function of Fuel Composition for U ₃ O ₈ -Al Metallothermic Reaction.....	39
20 Effect of U ₃ O ₈ Particle Size on Thermal Reactions in Rapidly Heated 53 wt % U ₃ O ₈ -Al Pellets	40
21 Comparison Between Time-Temperature Curves for a 53 wt % U ₃ O ₈ -Al Pellet and an Outer Tube Section Plunged into a Preheated Furnace.....	41
22 ORNL DTA Study of U ₃ O ₈ -Al Metallothermic Reaction.....	43
23 Exothermic Reaction Temperature for Uranium Oxides and Aluminum.....	44
24 Temperature of Slowly Heated Outer Tube Section with a 53 wt % U ₃ O ₈ -Al Core.....	46
25 Photomicrograph of Irradiated U ₃ O ₈ -Aluminum Tube Sections.....	48
26 Effect of Irradiation Temperature Upon the Extent of Reaction in the Cores of the Inner (Top) and Outer (Bottom) Annulus HFIR Fuel Plates	50
27 Relative Uranium and Aluminum Distribution Across a Typical Fuel Particle of an Irradiated U ₃ O ₈ Fuel Dispersion	51
28 Blister Temperature for Irradiated U ₃ O ₈ -Aluminum Fuel Tubes	55
29 Photographs of Blistered U ₃ O ₈ -Al Specimens.....	56
30 U ₃ O ₈ Particles Irradiated to 7.1×10^{21} Fissions/cc of U ₃ O ₈	58
31 Expected Fabrication Yield for U ₃ O ₈ -Al Fuel Tubes, Based on Developmental Tests	61
32 Strength of Partially Dissolved Uranium Oxide - Al Tubes (Vertical Mode).....	62
33 Reprocessing of Cermet Fuel Tubes.....	63

LIST OF TABLES

	PAGE
I Typical Particle Size Distribution for Roll Ground U ₃ O ₈	7
II Analyses of SRL U ₃ O ₈	11
III Comparison of Void Content in Rolled Plates and Extruded Tubes	14
IV Thermodynamic Properties of the Uranium Oxides.....	17
V Heat and Free Energy of Formation of Uranium Oxides.....	18
VI Average Axial Compressive Stress and Temperature to Collapse 53 wt % U ₃ O ₈ -Al and 35 wt % U-Al Outer Tubes in Air	30
VII Phase Assemblage Determined After Various Stages of the Powder Metallurgy Process.....	38
VIII Effect of Core Position on the U ₄ O ₉ Content of Vacuum Degassed Sample.....	38
IX SRL Irradiation Test of P/M Fuel Tubes	47
X Typical Wall Thickness Measurements for As-Extruded U ₃ O ₈ -Al Tubes (MK 14).....	53
XI Thickness Measurements for Tubes Irradiated to 5×10^{20} Fissions/cc Core.....	54
XII Thickness Measurements for Tubes Irradiated to 7×10^{20} Fissions/cc Core.....	54

PROPERTIES OF ALUMINUM- U_3O_8 CERMET FUEL

1.0 U_3O_8 -ALUMINUM FUEL

1.1 Introduction

Fuel elements for Savannah River Reactors consist of coextruded tubes that are about fifteen feet long. The tubes contain enriched uranium and aluminum alloy within the core of the element, and they are clad with 8001 aluminum alloy.

The current method for manufacturing fuel elements at the Savannah River Site (SRS) is to cast a uranium-aluminum alloy core, assemble the core into aluminum billet components, and coextrude the billet to produce tubular elements. Casting becomes difficult above about 35 wt% uranium.

Powder metallurgy (PM) provides an alternative way for manufacturing the core. The PM technique allows increased uranium content in extruded tubes. Fuel elements have been made with up to 60 wt% U_3O_8 (50 wt % U) in aluminum. Other advantages of the PM process include the ability for direct onsite uranium recycle at SRS, improved fabrication yield, reduced waste, increased product yield, and improved fabrication safety.

Oxide-aluminum dispersion fuel, sometimes called cermet fuel, has been used in research and test reactors in the U.S. and abroad. Some reactors using cermet fuel include the Puerto Rico Nuclear Center Reactor, the High Flux Isotope Reactor (HFIR), the High Flux Beam Reactor (HFBR), the National Bureau of Standards Reactor, and the Oak Ridge Research Reactor. Recently, several foreign countries have either built or converted existing reactors to U_3O_8 -aluminum fuel elements as part of the Reduced Enrichment of Research and Test Reactor Program.

This report documents parameters needed for reactor calculations and design of fuel elements containing U_3O_8 -aluminum for the New Production Reactor (NPR). Information was obtained from studies done at Savannah River Laboratory and from information cited in the literature.

1.2 Background of U_3O_8 -Aluminum Dispersion Fuels

The use of UO_2 or U_3O_8 dispersions in aluminum was first envisioned as a way to increase the uranium density beyond that fabricable with the U-Al alloy so that low enrichment uranium (20% ^{235}U) could be used for foreign and university reactors to reduce the risk of diversion and proliferation of highly enriched uranium (1). This effort eventually resulted in a core for the Puerto Rico Nuclear Center reactor of 65 wt% U_3O_8 in aluminum at 20% enrichment (2). The demonstration reactor for the 1955 Geneva Conference had been fabricated with UO_2 in aluminum but only with much difficulty due to swelling of the plates from the UO_2 -Al reaction (3). A lot of effort went into the study of the swelling reaction between UO_2 and Al which occurred during the brazing operation that was used to fasten the plates in the elements. The mechanism for the swelling was never completely understood; however, it could be avoided by the use of U_3O_8 which did not produce excessive swelling (4).

The period from about 1950 up to the development of the High Flux Isotope Reactor and the Advanced Test Reactor (ATR) in the early 1960's was very active for aluminum based fuel for research reactors (and other fuel and reactor types as well). The primary fuel materials examined at the Oak Ridge National Laboratory for increasing the uranium loadings beyond that which could be obtained with the U-Al alloy were: UO_2 , U_3O_8 , UC_2 , and alloy additions such as silicon to the U-Al alloy to promote the formation of UAl_3 rather than UAl_4 in the casting. Others such as UAl_2 , UC, and uranium silicides were mentioned in the progress reports briefly, but no substantial work on them was reported. As mentioned above, the swelling problem with UO_2 was never completely understood and solved. The severe reaction of UC_2 with water in defective plates made its use unattractive (5). The irradiation performance of both U_3O_8 and UAl_3 (cast material with silicon additions to promote UAl_3) dispersions in aluminum was satisfactory (6).

Both U-Al alloy and U_3O_8 dispersions were considered for the HFIR. The U_3O_8 dispersion was chosen because of improved homogeneity control, core configuration control, less problems with blisters and bonding during rolling, and the ability to reproducibly add boron (as boron carbide) as distributed burnable poison (7). "Dead-burned" oxide and "High-fired" (8) oxide were tested and performed satisfactorily both in fabrication and irradiation (9). The high-fired U_3O_8 is more resistant to fragmentation during rolling and gave more reproducible results for the homogeneity tests and ultrasonic bonding tests and thus was selected for the plate fabrication (10).

The original development work on the ATR elements at ORNL also used U_3O_8 dispersions mainly for the same reasons as for HFIR (9). The Idaho National Engineering Laboratory later chose UAl_x dispersions produced by powder metallurgy for the ATR fuel.

Later, when commercial suppliers of U-Al alloy fuel were no longer available, research reactors which used this fuel were forced to switch to an alternative. Reactors which obtained their fuel through ORNL switched to the U_3O_8 dispersion which was being used for the HFIR. Reactors which obtained their fuel through INEL switched to the UAl_x dispersion which was being used for the ATR.

2.0 PHYSICAL AND MECHANICAL PROPERTIES

Dispersion fuels for nuclear reactors have fuel-bearing particles uniformly dispersed in a well behaved metal matrix. To minimize radiation damage and provide metallic properties, the matrix must predominate in volume and exist as a continuous phase surrounding the fissile material. The fuel element core or meat section is made using PM techniques.

Selection of the fuel form involves evaluating the irradiation stability of the compound at high temperature and the physical and mechanical properties such as strength, density, and melting point. The matrix material for fuel elements is selected from metals that are strong, ductile, and insensitive to neutron damage. Some requirements include high thermal conductivity, low coefficient of thermal expansion, and low neutron absorption cross-section. Physical and mechanical properties of U_3O_8 and aluminum will be reviewed in the following sections.

2.1 Composition

A diagram is shown in Figure 1 for the manufacture of reactor fuel tubes by the powder metallurgy process at the Savannah River Site (SRS). The basic process includes powder preparation, billet core compaction, and tube coextrusion. Steps in these areas will be briefly discussed.

2.1.1 Powder Preparation

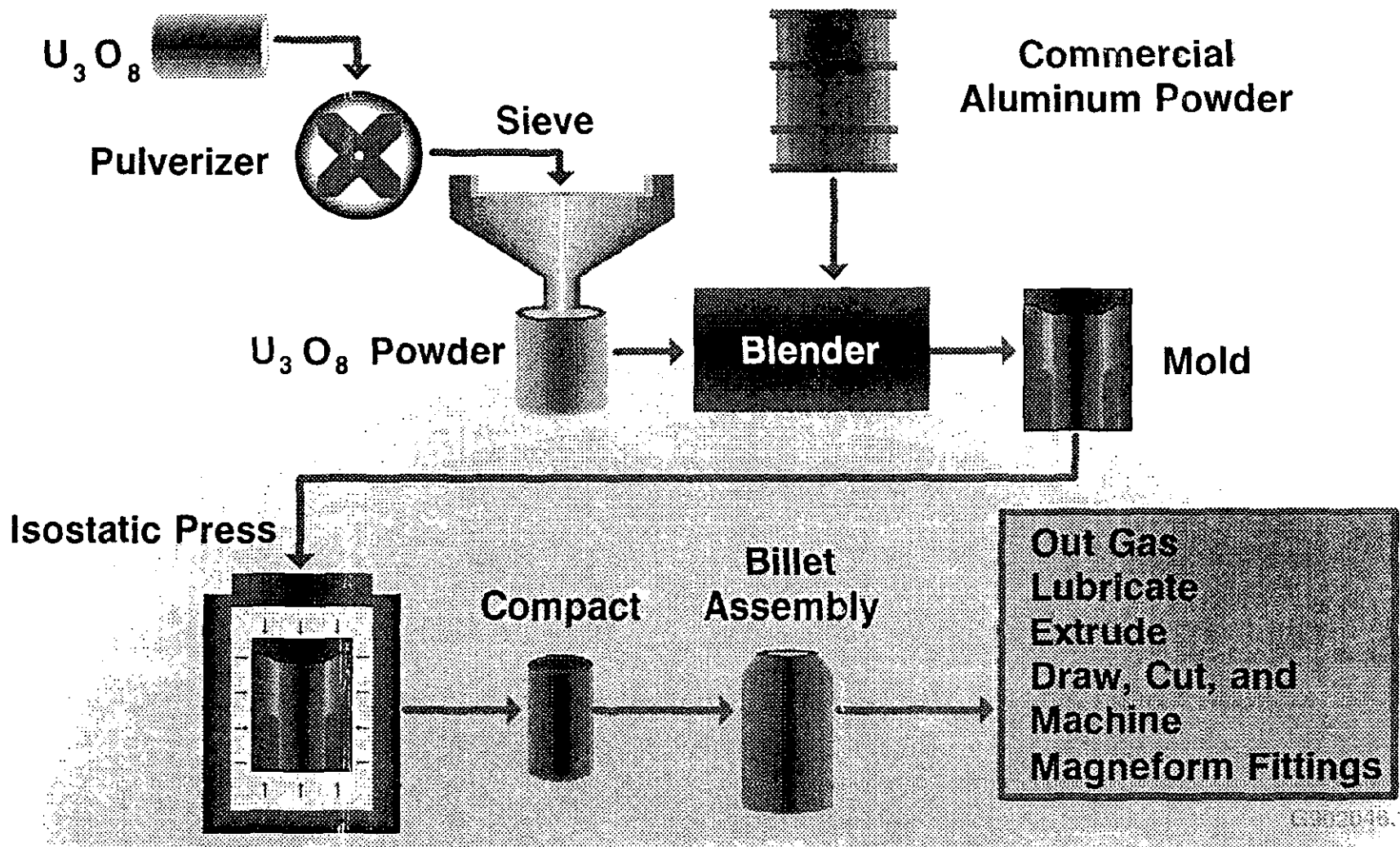
Uranium Oxide (U_3O_8) has been made for nuclear reactors using several different techniques. Oak Ridge developed an oxide for the High Flux Isotope Reactor which uses the peroxide precipitation process⁽¹¹⁾. The precipitate is calcined at 800°C in a low-grade nitrogen atmosphere, sized and then calcined again at 1400°C in air. This process produces a sintered oxide particle that is strong but friable. The oxide is designated as high-fired U_3O_8 .

Oak Ridge also developed a burned U_3O_8 . This oxide is made using uranium metal turnings. The turnings are put into a furnace, ignited, and allowed to burn. Oxygen is added near the end of the process to ensure complete oxidation of the uranium metal. The irradiation performance of the burned oxide is as good or better than that of high-fired oxide.

For process development at SRS, denitrated UO_3 was obtained from Oak Ridge Y-12 Plant and calcined to U_3O_8 at 800°C in an electric furnace⁽¹²⁾. A low-grade nitrogen atmosphere was used during calcining. The UO_3 oxide was produced by continuous denitration during the conversion of uranyl nitrate hexahydrate (UNH) solution to uranium metal^(13,11). The average particle size of the UO_3 from Y-12 was about 800 microns in diameter. SRS is currently building a Fuel Solidification Facility (FSF) to convert UNH solution to UO_3 on site⁽¹⁴⁾. This material can be easily converted to U_3O_8 on plant for on-site uranium recycle.

The SRS U_3O_8 powder calcined at 800°C is shown in Figure 2. A low grade nitrogen atmosphere was used, but it is not necessary because U_3O_8 is the stable phase when UO_3 is calcined in air at temperatures above 570°C⁽¹⁵⁾.

Oxide particles produced from denitration of uranyl nitrate consist of an agglomeration of smaller particles. In Figure 2b, the average particle size in the agglomerates is estimated to be about 1 micron.

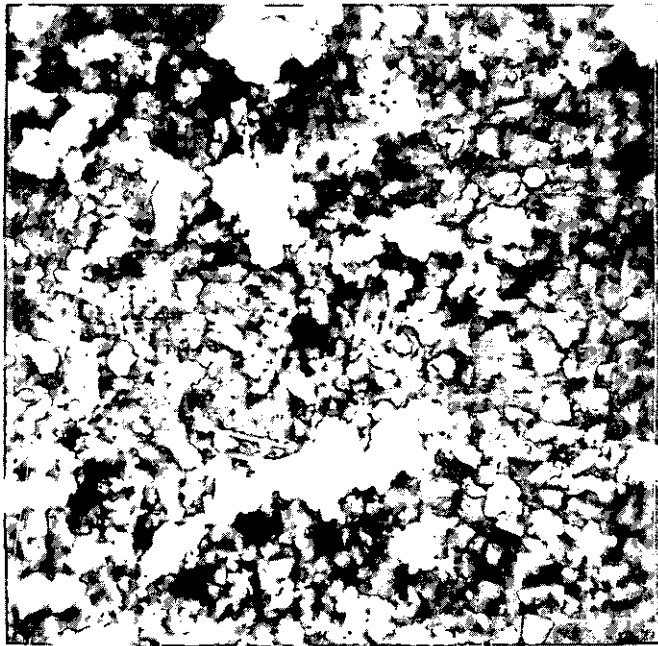


- 4 -

FIGURE 1. POWDER METALLURGY PROCESS AT SRS



(a) 50X



(b) 5000X

FIGURE 2. TYPICAL PHOTOMICROGRAPHS FOR U_3O_8 PRODUCED BY CALCINING UO_3 AT $800^\circ C$ IN A LOW GRADE NITROGEN/AIR ATMOSPHERE

2.1.2 Grinding

The U_3O_8 powder is ground to produce an acceptable particle size distribution for the PM process. Particle-size distribution is one of the most important parameters for producing good blends of U_3O_8 and aluminum powders. If the size distribution is outside specified limits, complete separation of the powders can occur during blending. Roll grinding has been used at SRS in the past to produce the acceptable distribution given in Table I. Powders normally contain about 40 wt% fine particles (< 44 microns in diameter).

2.1.3 Blending

By blending ground U_3O_8 and commercial Alcoa 101 aluminum powder, a homogeneous mixture of the oxide fuel in aluminum can be achieved. Test results shown in Figure 3 indicate that the coefficient of variation (CV) for a 40 wt% blend is about 5% after only 100 revolutions of the blender. At 20 rpm, this would take 5 minutes of blending. However, powders are normally blended for 10 minutes to ensure proper mixing.

The coefficient of variation is defined as the standard deviation of thieved samples expressed as a percentage of the mean oxide content. A CV of 5% corresponds to a standard deviation of 2% in uranium oxide per 0.25 x 0.25 inch section of the core for a 40 wt% oxide fuel tube. This is at the 95% confidence level.

2.1.4 Compaction

After blending, powder is placed in an elastomeric bag for isostatic compaction. Compaction is carried out in water at room temperature. Pressures up to 30,000 psi have been used to produce billet cores. The compacted core is placed inside aluminum billet components for single coextrusion. The coextrusion process produces an aluminum clad tube which contains the aluminum-oxide fuel mixture in the core section. The cladding is 8001 aluminum alloy.

2.1.5 Coextrusion

Tubes have been extruded successfully, on a production basis, with up to about 60 wt% oxide. The extrusion ratios have varied from about 24 to 30. Extrusion is done at billet temperatures above 400°C.

At 60 wt%, the oxide phase constitutes about 28% of the volume. Longitudinal and transverse sections of an extruded tube containing 80 and 59 wt% oxide are shown in Figure 4. Large oxide particles (>60 microns) tend to crack during extrusion of tubular elements. Cracking is observed perpendicular to the longitudinal direction because large tensile strains (>300%) occur along the tube axis in the extrusion direction. Cracks are not as apparent in the transverse section because a compressive stress acts in the radial direction as the material moves through the extrusion die.

TABLE I
TYPICAL PARTICLE SIZE DISTRIBUTION FOR ROLL GROUND U₃O₈

Mesh Size	Spherical Diameter, um	Wt %
-100/+140	105-150	22
-140/+170	88-104	9
-170/+200	74-87	10
-200/+270	53-73	15
-270/+325	44-52	4
-325	<44	40

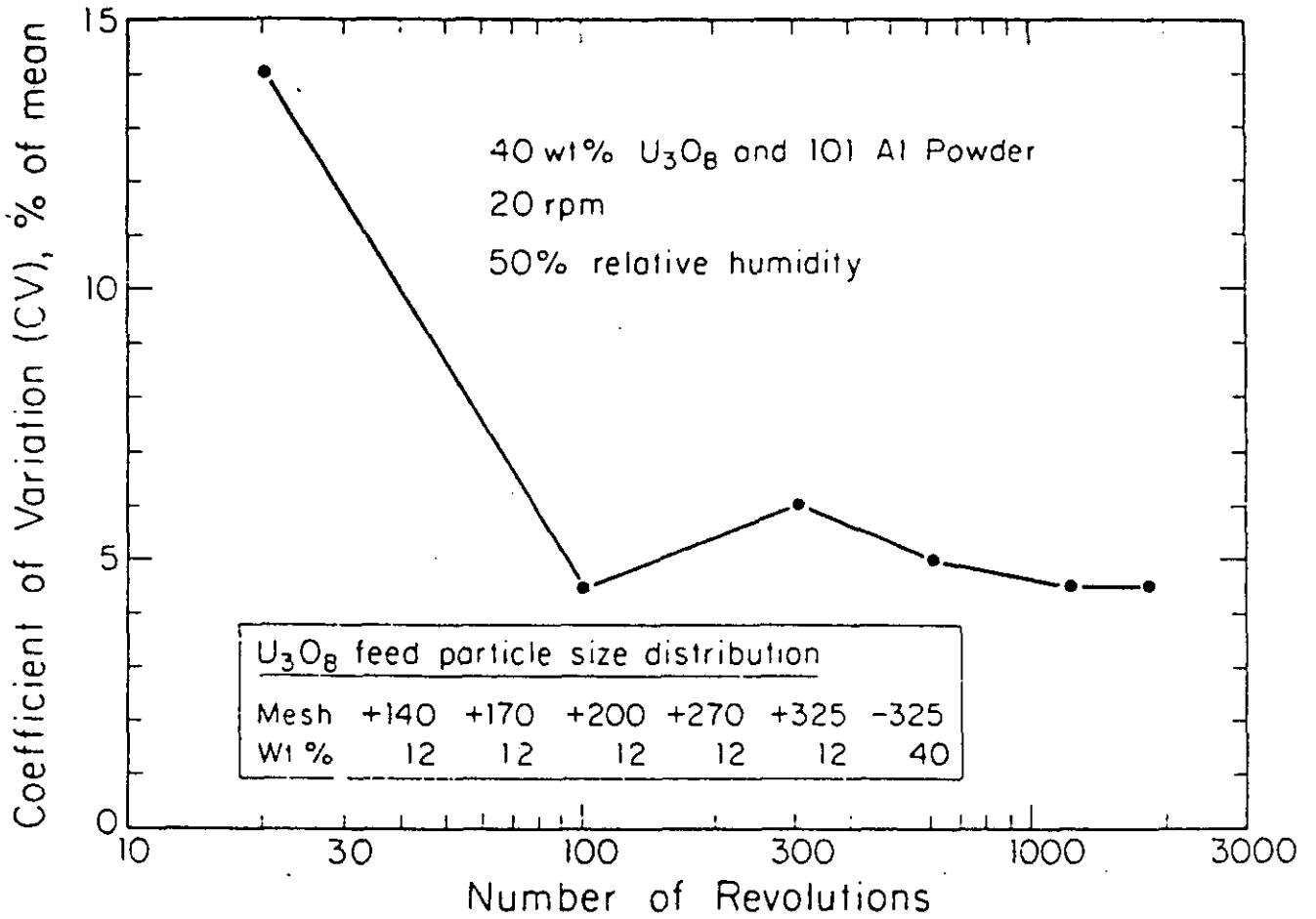
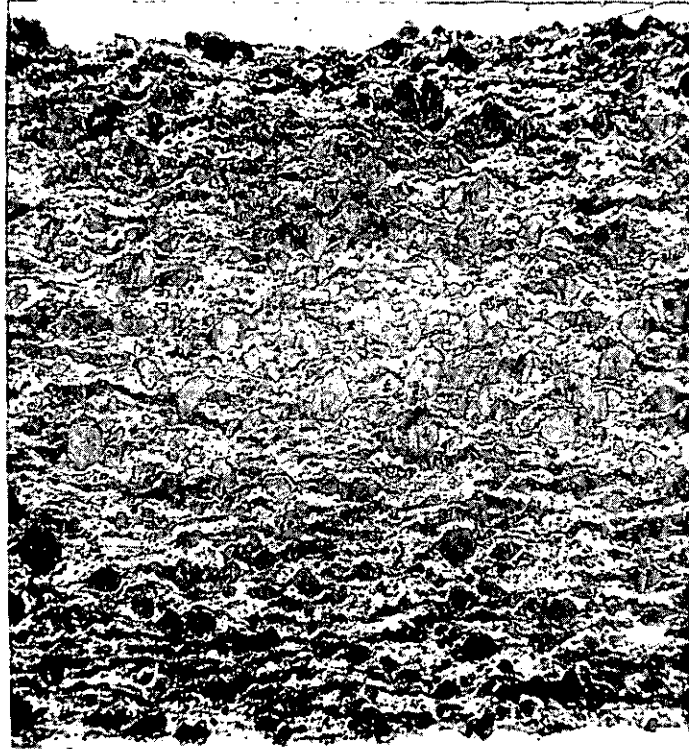
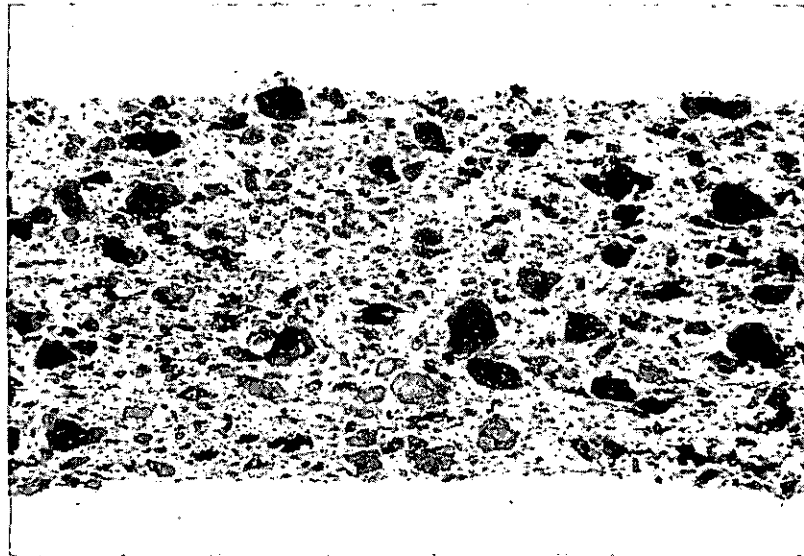


FIGURE 3. TEST OF MODIFIED TUMBLING MIXER

Reference: Peacock, H. B., "Powder Metallurgy at Savannah River Laboratory,"
 E. I. du Pont de Nemours and Company, DP-1524, December 1978



a) Longitudinal Section, 80 wt% 38X



b) Transverse Section, 59 wt% 50X

FIGURE 4. LONGITUDINAL AND TRANSVERSE SECTIONS FROM AN EXTRUDED U_3O_8 -Al FUEL TUBE CONTAINING 80 WT % AND 59 WT % OXIDE

The transverse section shows a uniform distribution of oxide particles in the aluminum matrix. During high temperature outgassing and extrusion, U_3O_8 powder is reduced to U_4O_9 (16, 17). Studies indicate that as much as 50% reduction takes place. No $UAlx$ products have been detected until extruded sections were heated at about 600°C for 12 hours (16).

2.1.6 Rolling

Fuel elements for several different research and test reactors are made using hot rolling techniques(18, 19). The basic procedure consists of cold pressing a green compact at about 30 tsi. Frames and cover plates of 6061 aluminum alloy are cleaned in caustic for roll bonding. The compact is placed inside the frame and the cover plates welded in place. The assembly is degassed. Bonding the cladding to the frame and compact is done by hot rolling at 490°C to an 85% reduction in thickness. The plate is then annealed at 490°C for 1 hour to soften and test for blistering. Plates are then cold rolled (10%) and heat treated to "O" temper for the 6061 alloy.

2.2 Density

Density is defined as the mass per unit volume. The density of elements or compounds can be determined experimentally or calculated from x-ray diffraction data.

2.2.1 Powders

The density of U_3O_8 was found pycnometrically by Gronvold(20) to be 8.34 gm/cc. Calculations indicated a density of 8.42 gm/cc(20). The generally accepted value for the theoretical density of U_3O_8 ($UO_{2.67}$)(21) is 8.3.

Particle density for U_3O_8 produced at SRS was determined using a helium pycnometer and compared with density measurements made using a manual toluene pycnometer(22). Data agreed within 2%. The U_3O_8 oxide was produced by calcining UO_3 which was made by continuous denitration at Oak Ridge Y-12. The density was 7.0 gm/cc when calcined in low-grade nitrogen and 7.3 g/cc when calcined in air. The density difference indicates about a 4% larger void fraction for UO_3 calcined in a nitrogen atmosphere. Firing the UO_3 in nitrogen for 6 hours at 800°C produced particles having about 83% of the theoretical density.

The particle surface area is also shown in Table II for U_3O_8 oxide made at Savannah River Laboratory. The surface area was determined by gas adsorption BET (Brunauer-Emmet-Teller) method using krypton gas(22). The surface area was 0.09 m²/g and 0.17 m²/g for U_3O_8 powder produced at 800°C in flowing, low-grade, nitrogen and air atmospheres, respectively. About 75% of the difference in surface area was attributed to differences in the average particle size of the two powder samples.

TABLE II
ANALYSES OF SRL U₃O₈

Description	gU/g	Surface Area (a) m ² /g	Particle Density (g/cc)	
			He Disp. (b)	Toluene (c)
U ₃ O ₈ , 800°C 6 hrs in N ₂	0.84364	0.09	6.99	6.87
U ₃ O ₈ , 800°C 6 hrs in air	0.84397	0.17	7.30	7.26

- (a) BET using krypton.
- (b) Micrometrics, helium displacement automatic pycnometer.
- (c) Toluene displacement - manual pycnometer.

Reference: Peacock, H. B., "Preparation and Physical Properties of U₃O₈,"
E. I. du Pont de Nemours and Company, DPST-83-276, January 1983

2.2.2 Extruded Tubes

Billet cores are compacted at room temperature in a high-pressure water isostat. Isostatic pressures range up to 30,000 psi. After compaction, the billet cores are assembled into aluminum components for coextrusion at temperatures above 400°C. Extrusion forces vary from 600 to 900 tons which depend on size and shape of the tube extruded.

During extrusion, large three-dimensional strains⁽²³⁾ occur as the material flows through the conical die. These strains produce densification and cause tensile cracking of oxide particles. These cracks produce fabrication voids within the core.

The total void content for extruded tubes was calculated from tube density measurements. The density was determined experimentally using Archimedes' principle of water immersion⁽²⁴⁾. Figure 5 shows the void fraction as a function of wt% U_3O_8 for extruded tubes having a roll ground oxide distribution. Oxide particle size distribution affects the void content because particles less than about 60 microns tend not to crack during the extrusion operation. The average value for the void content is estimated from the data to be within $\pm 20\%$.

The void content for extruded tubes increases as the oxide content increases and is an approximate linear function of loading up to 60 wt% oxide. For extruded tubes, the average void fraction varies from 0.06 at 20 wt% to about 0.15 at 60 wt% U_3O_8 . Above 60 wt% oxide, stringers form along the tube axis resulting in more fabrication voids and a non linear increase in the tube void fraction. Voids are useful in reactor fuel elements because they are sites where fission gases can accumulate and thus reduce tube swelling.

For comparison, the void fraction is given in Table III for ORNL's HFIR and burned U_3O_8 in hot rolled plates^(25, 26) and SRS's calcined U_3O_8 in extruded tubes. SRS extruded tubes contain almost twice the void fraction of rolled HFIR plates. Plates containing burned oxide have almost 1.5 times the void fraction of HFIR elements, which accounts for its good irradiation performance.

Void fraction is a function of oxide type and content. Differences in void content between rolled and extruded fuel elements having similar type oxides is most likely related to the stress distribution produced during the fabrication operation. A higher longitudinal tensile stress is expected during extrusion.

The volume fractions of aluminum, U_3O_8 , and voids for extruded tubes containing SRS type oxide are summarized in Figure 6. The volume fraction is plotted as a function of weight percent oxide. Also shown on the figure is the grams per cubic centimeter of uranium expected for extruded tubes. At the 60 wt% U_3O_8 , the expected uranium loading is 1.95 g/cc.

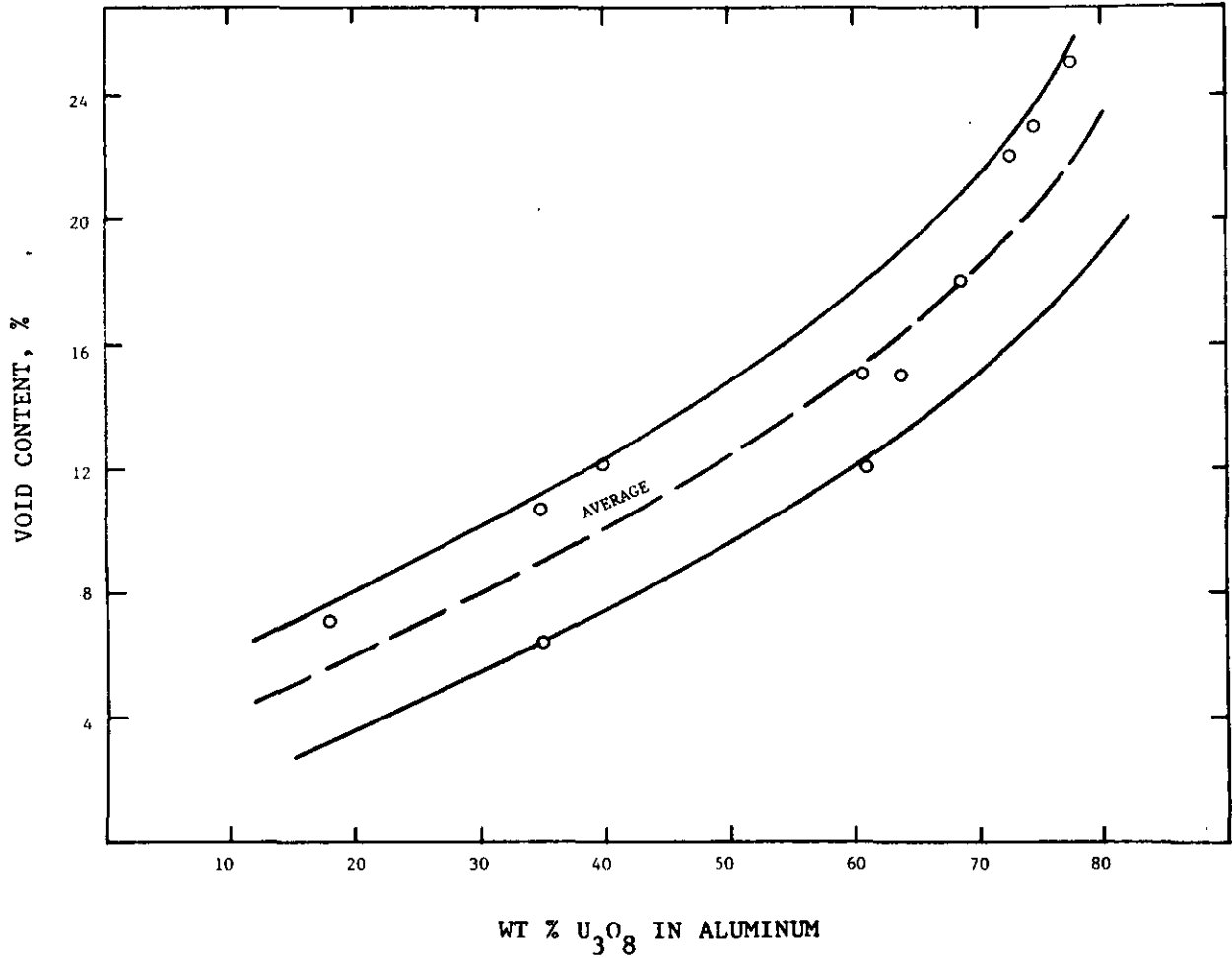


FIGURE 5. VOID CONTENT FOR EXTRUDED REACTOR FUEL TUBES CONTAINING U₃O₈ AND ALUMINUM

Reference: Peacock, H. B., A Technique to Determine Billet Core Charge Weight for PM Fuel Tubes, E. I. du Pont de Nemours and Company, DPST-84-516, 1984

TABLE III
COMPARISON OF VOID CONTENT
IN ROLLED PLATES AND EXTRUDED TUBES

Wt % U ₃ O ₈	Vol % U ₃ O ₈	VOID FRACTION		
		Rolled Plates (1)		Extruded Tubes
		HFIR	Burned	800°C Calcined UO ₃
32	12	.03	~.05	.08
40	16	.04	.06	0.10
50	21	.05	.08	0.12
65	31	.07 (2)	-	0.16
70	35	.09 (2)	-	0.18
75	39	0.11 (2)	-	0.20

References:

1. Martin, M. M., Monthly Report, ORNL 4600, p. 244, June 1970.
2. Copeland, G. L. and Martin, M. M., "Fabrication of High-Uranium-Loaded U₃O₈-Al Developmental Fuel Plates," ORNL/TM-7607, December 1980.

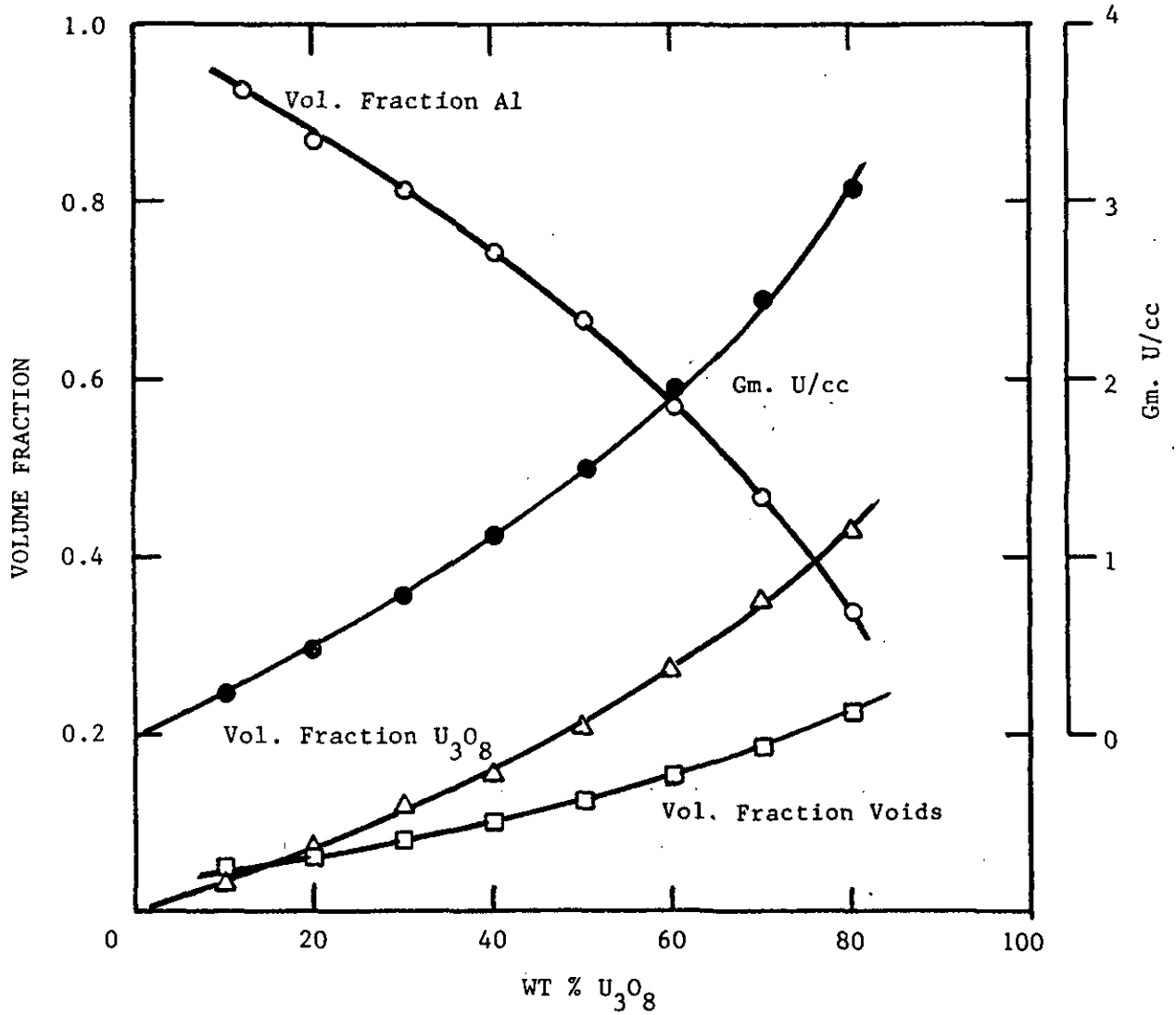


FIGURE 6. ALUMINUM AND URANIUM OXIDE VOLUME FRACTIONS AND TUBE LOADINGS FOR EXTRUDED PM FUEL TUBES

2.3 Thermodynamic Properties

Thermodynamic properties of the uranium oxides have been determined by Brewer⁽²⁴⁾. He used results obtained by Jones, Gordon, and Long⁽²⁷⁾ along with data from Huber, Holley, and Meierkord⁽²⁸⁾ to calculate the heats of formation, free energy, and entropy at 298°K for various oxides. The results of the calculations are presented in Table IV.

Coughlin⁽²⁹⁾ calculated ΔH and ΔF values for the formation of UO_2 , U_3O_8 and UO_3 between 298°K and 1500°K while Glassner⁽³⁰⁾ listed constants for the evaluation of the thermodynamic properties of uranium oxides up to 2500°K. The data are shown in Table V.

2.3.1 Specific Heat

Specific heat measurements for U_3O_8 were carried out by Popov, Gal'chenko, and Senin⁽³¹⁾. Studies were done in a platinum calorimetric vessel. The heating rate was 1° per 78-80 seconds and 1° per 113-115 seconds. The data was summarized by the equations

$$C_p = 53.51 + 8.99 \times 10^{-2} T - 1.229 \times 10^{-4} T^2$$

in the temperature range of 100 to 320°C and

$$C_p = 64.25 + 1.582 \times 10^{-2} T$$

in the temperature range of 400 to 600°C.

Curves for the specific heats for aluminum and U_3O_8 have been published by Touloukian⁽³²⁾ and are given in Figure 7.

The specific heat for mixtures of U_3O_8 and aluminum has not been determined. For mixtures, the specific heat can be calculated using the ideal mixing equation. The molar specific heat is given by

$$C_{p,U_3O_8-Al} = (C_{p,U_3O_8})(\text{Mol wt.})(M\%) + C_{p,Al}(26.98)(1.00 - M\%)/100$$

2.4 Thermal Conductivity

Heat is generated within the fuel particles and is conducted through the wall to the cooling medium. The conduction of heat depends on the thermal conductivity of the material. The thermal conductivity is define as the amount of heat that will flow across a unit area if the temperature gradient is unity.

TABLE IV
THERMODYNAMIC PROPERTIES OF URANIUM OXIDES

Compound	$-\Delta H_{298}$ (kcal per gram- atom uranium)	$-\Delta F_{298}$ (kcal per gram- atom uranium)	$-\Delta S_{298}$ (cal per gram- atom uranium per ° C)
UO ₂	259.2	246.6	43.4
UO _{2.25}	270.0	256.6	(47)
UO _{2.62}	285.6	269.9	(55)
UO _{2.67}	284.5	268	55.4
α UO ₃	291	273	62.1

Reference: Brewer, L., "The Thermodynamic Properties of the Oxides and Their Vaporization Processes," Chem. Revs. 52, 1-75, 1953

TABLE V
HEAT AND FREE ENERGY OF FORMATION OF URANIUM OXIDES

Temp (°K)	UO ₂		UO _{2.67}		UO ₃	
	-ΔH(±0.6)	-ΔF(±0.7)*	-ΔH(±0.5)	-ΔF(±1.2)*	-ΔH(±5)*	-ΔF(±5)*
298.16	259.2	246.6	284.5	268.0	291.0	272.5
400	258.9	242.3	284.2	262.4	290.5	266.0
500	258.6	238.2	283.9	257.0	290.5	260.0
600	258.3	234.1	283.6	251.6	290.0	254.0
700	258.0	230.1	283.3	246.3	290.0	248.0
800	257.8	226.1	283.1	241.0	289.5	242.5
900	257.6	222.1	282.9	235.8	289.5	236.5
935	357.6	220.7	282.9	234.0	289.5	234.5
935	258.3	220.7	283.6	234.0	290.0	234.5
1000	258.2	218.1	283.4	230.5	290.0	230.5
1045	258.1	216.3	283.4	228.1	290.0	228.0
1045	259.2	216.3	284.5	228.1	291.0	228.0
1100	259.1	214.1	284.3	225.2	291.0	224.5
1200	258.8	210.0	284.0	219.8	290.5	218.5
1300	258.4	206.0	283.7	214.5	290.5	212.5
1400	258.1	201.9	283.3	209.2	290.0	206.5
1405	258.1	201.7	283.3	208.9	-----	-----
1405	261.3	201.7	286.5	208.9	-----	-----
1500	261.1	197.7	286.3	203.7	-----	-----

*ΔH and ΔF in kcal per gram-atom uranium

Reference: Caughlin, J. P., "Heats and Free Energy of Formation of Inorganic Oxides,"
U. S. Bureau of Mines Bull. 542, 1954.

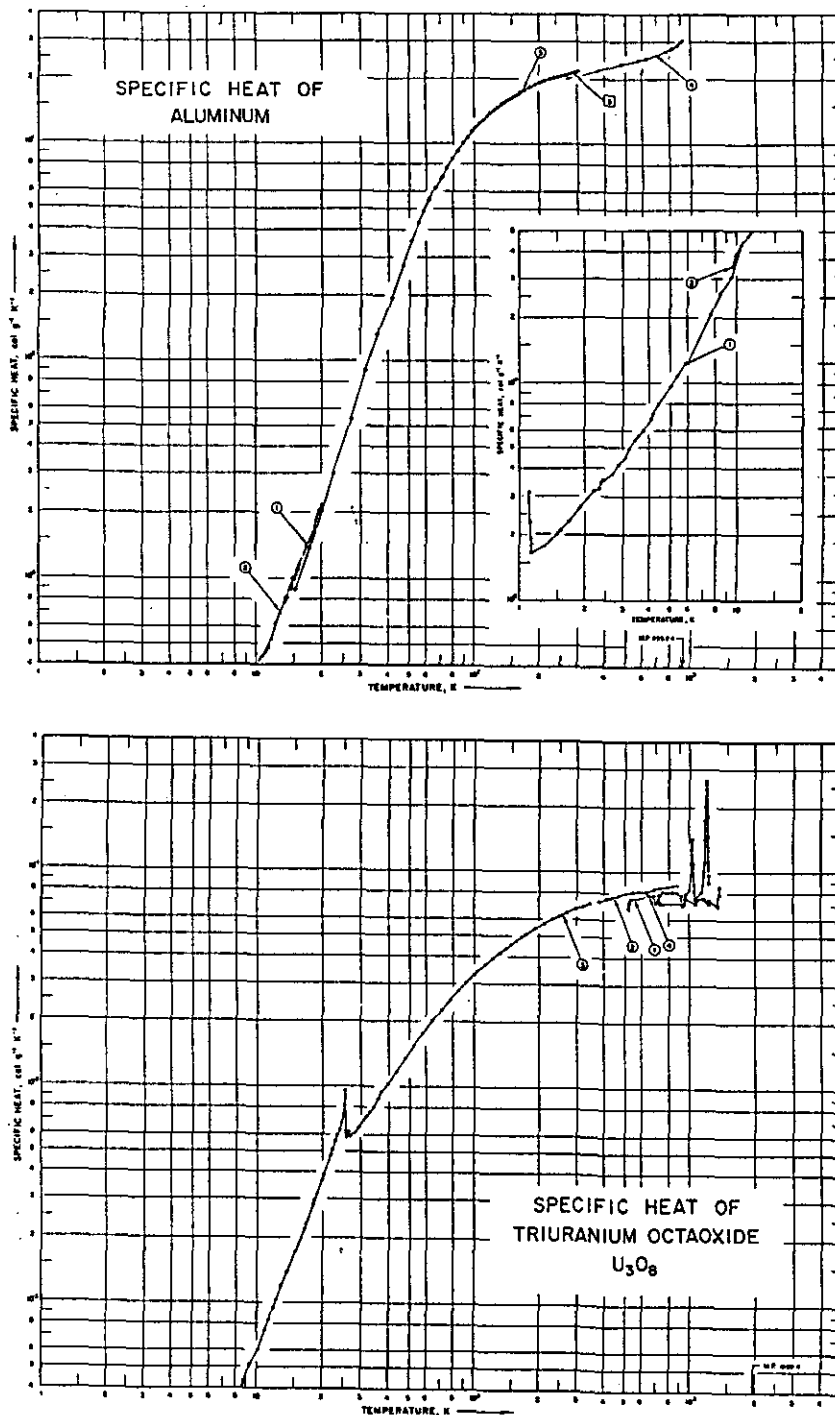


FIGURE 7. SPECIFIC HEAT OF ALUMINUM AND TRIURANIUM OCTAOXIDE (U₃O₈)

Reference: Touloukian, V. S. (dir), Thermophysical Properties of Matter, The TPRC Data Series, Volumes 4 and 5

2.4.1 Uranium Octaoxide (U₃O₈)

The thermal conductivity of several polycrystalline uranium oxides in the UO₂-U₃O₈ region was measured at 60°C by Ross⁽³³⁾. All the thermal conductivities reported were corrected to zero porosity by the simplified Loeb equation

$$K_m = K_T(1-P)$$

where K_m is the thermal conductivity of the mixture including pores, K_T is the theoretical value of the thermal conductivity and P is the fractional pore volume.

Thermal conductivities of non-stoichiometric uranium oxides relative to that for stoichiometric UO₂ are shown in Figure 8. Data in this figure are compared with data obtained by Belle⁽³⁴⁾ and Nichols⁽³⁵⁾ and show good agreement. Samples having compositions between UO₂ and UO_{2.21} were shown to consist of UO₂ containing a precipitated U₄O₉ phase. The thermal conductivity decreases with increasing oxygen-to-uranium atomic ratio. The decrease was attributed to the U₄O₉ phase having a lower thermal conductivity than the parent UO₂. The thermal conductivity of polycrystalline U₃O₈ samples was approximately 25 percent of that for stoichiometric UO₂.

The change in thermal conductivity of U₃O₈ with increasing temperature was determined by Schulz⁽³⁶⁾, and is shown in Figure 9. Thermal conductivity of U₃O₈ decreased linearly from about 0.028 W/cmK at 365°K(92°C) to 0.020 W/cmK at 750°K(477°C). The rate of decrease in the thermal conductivity was 2.08×10^{-5} per degree K, and the total percent change was about 28% over the temperature range.

2.4.2 U₃O₈-Aluminum Mixtures

Cermet reactor fuel elements are formed by mixing U₃O₈ and aluminum powders and then mechanically fabricating either tubular or plate elements. The microstructure consists of oxide particles imbedded in an aluminum matrix as shown in Figure 4. The thermal conductivity of the oxide phase is much less than for the aluminum matrix.

The thermal conductivity for mixtures of U₃O₈ and aluminum was calculated⁽³⁷⁾ using Buggerman's equation for isotropic mixtures⁽³⁸⁾. The relationship is given by

$$P_1 \frac{K_1 - K_m}{K_1 + 2K_m} + P_2 \frac{K_2 - K_m}{K_2 + 2K_m} = 0$$

where K_1 and K_2 are the conductivity of the phases present in the mixture and K_m the conductivity of the total aggregate. P_1 and P_2 represents the volume percent of the phases present in the mixture. Results from the calculations are presented in Figure 10 where the ratio of the thermal conductivity of the mixture to the thermal conductivity of aluminum is given as a function of weight percent oxide.

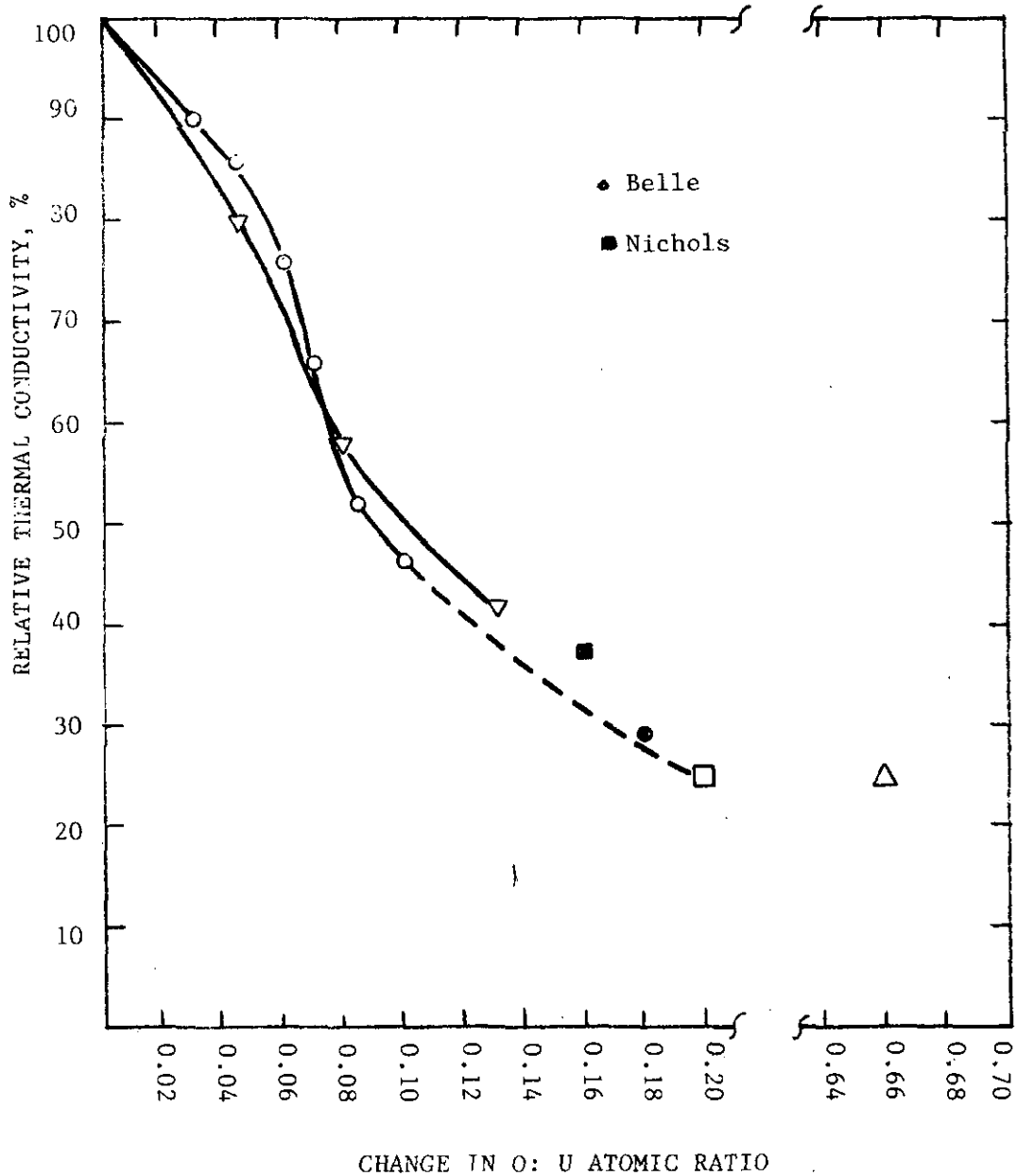


FIGURE 8. THERMAL CONDUCTIVITIES OF NON-STOICHIOMETRIC URANIUM OXIDES RELATIVE TO THAT FOR STOICHIOMETRIC UO₂

Reference: Ross, A. M., "The Dependence of the Thermal Conductivity of Uranium Dioxide on Density, Microstructure, Stoichiometry and Thermal-Neutron Irradiation," Atomic Energy of Canada, AECL-1096 (CRFD-817), September 1960

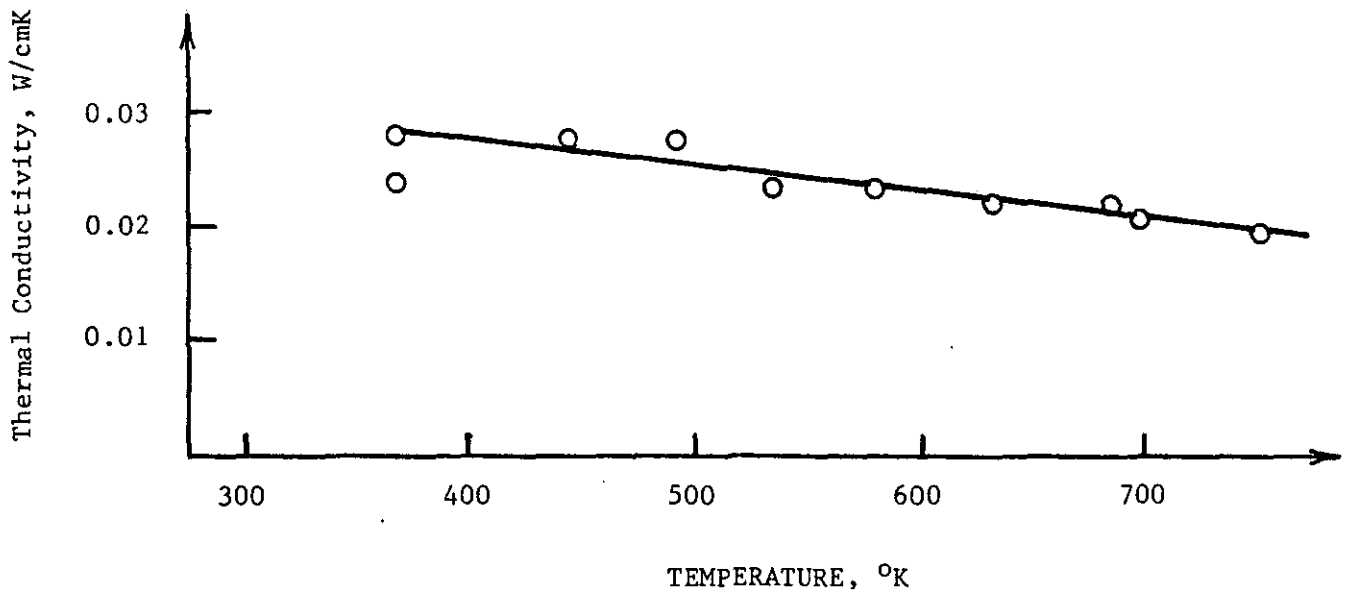


FIGURE 9. EFFECT OF TEMPERATURE ON THE THERMAL CONDUCTIVITY OF U_3O_8

Reference: Schulz, B., "Anomalie Der Thermischen Ausdehnung Und Wärmeleitfähigkeit Von U_3O_8 ," Rev. int. Htes Temp. et Refract. 12, pp 132-134, 1975

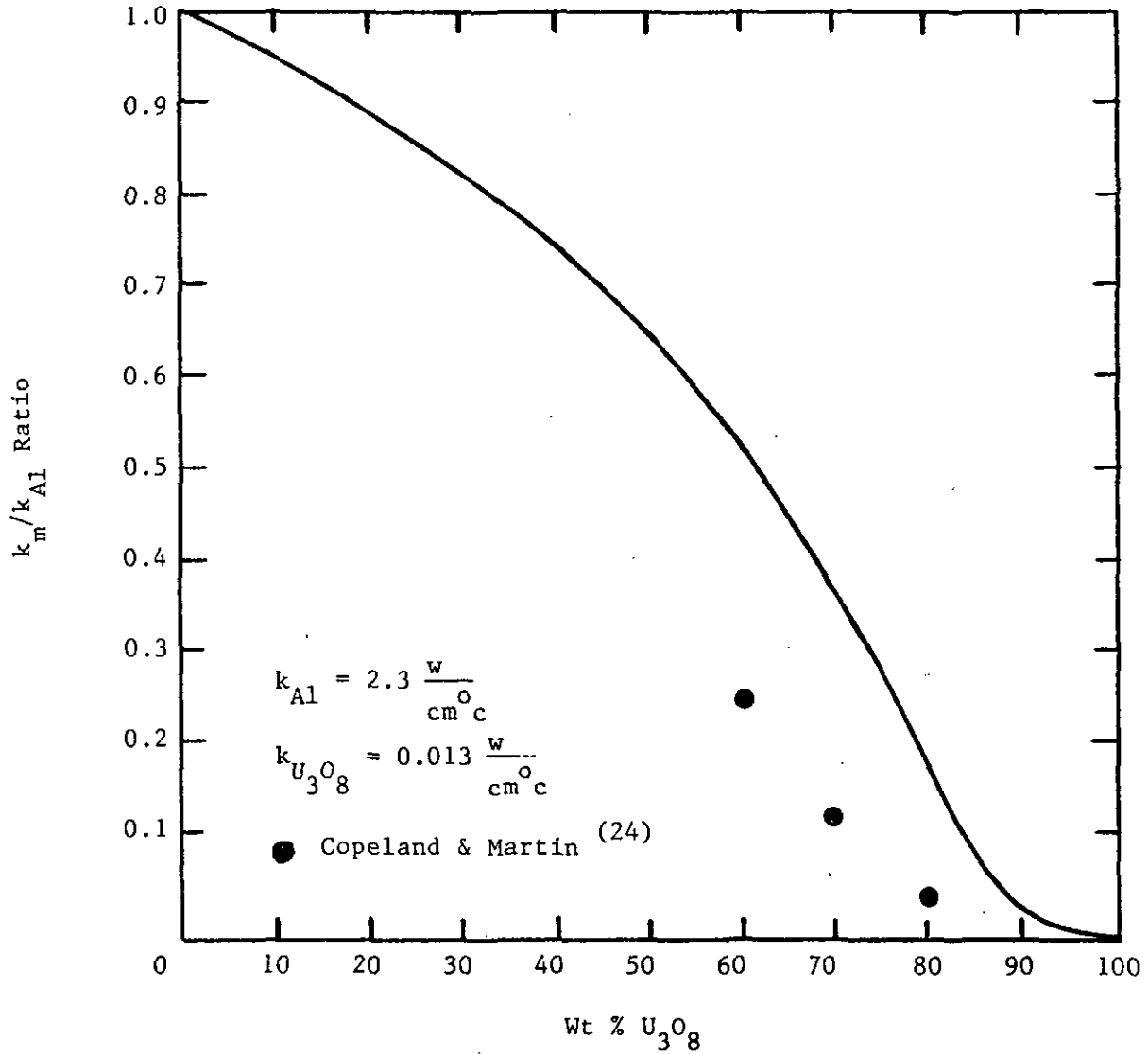


FIGURE 10. CALCULATED THERMAL CONDUCTIVITY RATIO (k_m/k_{Al}) FOR U_3O_8 /ALUMINUM MIXTURES

Reference: Peacock, H. B., Thermal Conductivity of U_3O_8 -Al Mixtures, E. I. du Pont de Nemours and Company, DPST-79-349, 1979

Copeland and Martin⁽³⁹⁾ measured the thermal conductivity of cermet fuel plates containing 60 to 80 wt% U_3O_8 in aluminum and clad in 6061 aluminum. At 60 wt% oxide the thermal conductivity was measured to be about $0.55 \text{ W/cm}^2\text{C}$ while at 80 wt% oxide the thermal conductivity decreased to about $0.08 \text{ W/cm}^2\text{C}$. Data for 60, 70, and 80 wt% U_3O_8 are plotted in Figure 10. Experimental values for the thermal conductivity ratio are lower than the calculated values by 18-47%.

Reasons for the difference between the calculated and measured values may be due to the fact that fabrication porosity was not considered in the calculations of the thermal conductivity. Calculated values do not include the thermal conductivity of the cladding material. Also the equations may be less accurate at intermediate oxide concentrations.

Irradiation tends to reduce the thermal conductivity of the oxide, probably due to the microstructure of the irradiated oxide particles. Point defects are produced and sintering of voids occur producing a somewhat uniform pore distribution within the particles as will be shown in a later section.

The effect of thermal neutron irradiation has been determined for UO_2 ⁽³³⁾. After an irradiation to approximately $2 \times 10^{17} \text{ n/cm}^2$, the thermal conductivity decreased about 26%. Longer irradiation time appeared to cause no further decrease in thermal conductivity. If the decrease is related to the formation of defects and sintering of voids, then a similar decrease would be expected for U_3O_8 . However, reactions with aluminum during irradiation may affect the composition and alter the thermal conductivity. The solidstate reaction products expected are UAl_x , Al_2O_3 , U_4O_9 , and UO_2 .

2.5 Linear Expansion

The linear expansion of U_3O_8 in the pressing direction was measured by Schulz⁽³⁶⁾ for the temperature range 293°K to 1063°K . The samples were pressed to about 80% theoretical density. Expansion curves, shown in Figure 11, from 373°K (100°C) up to 623°K (350°C) showed negative values while above 623°K positive values were obtained. The results were related to known data for phase-transition-temperatures of the orthorhombic U_3O_8 .

Thermal expansion has not been determined for cermets containing U_3O_8 and aluminum. But, based on the thermal expansion data for U_3O_8 , it is expected that the thermal expansion of the cermet element would correspond to the expansion of aluminum. In a fabricated cermet element, there appears to be no chemical bonding between the ceramic oxide phase and the aluminum matrix. Uranium oxide shows a thermal contraction below the melting point of aluminum which would create additional voids in the matrix for fuel temperatures less than about 900°K (627°C).

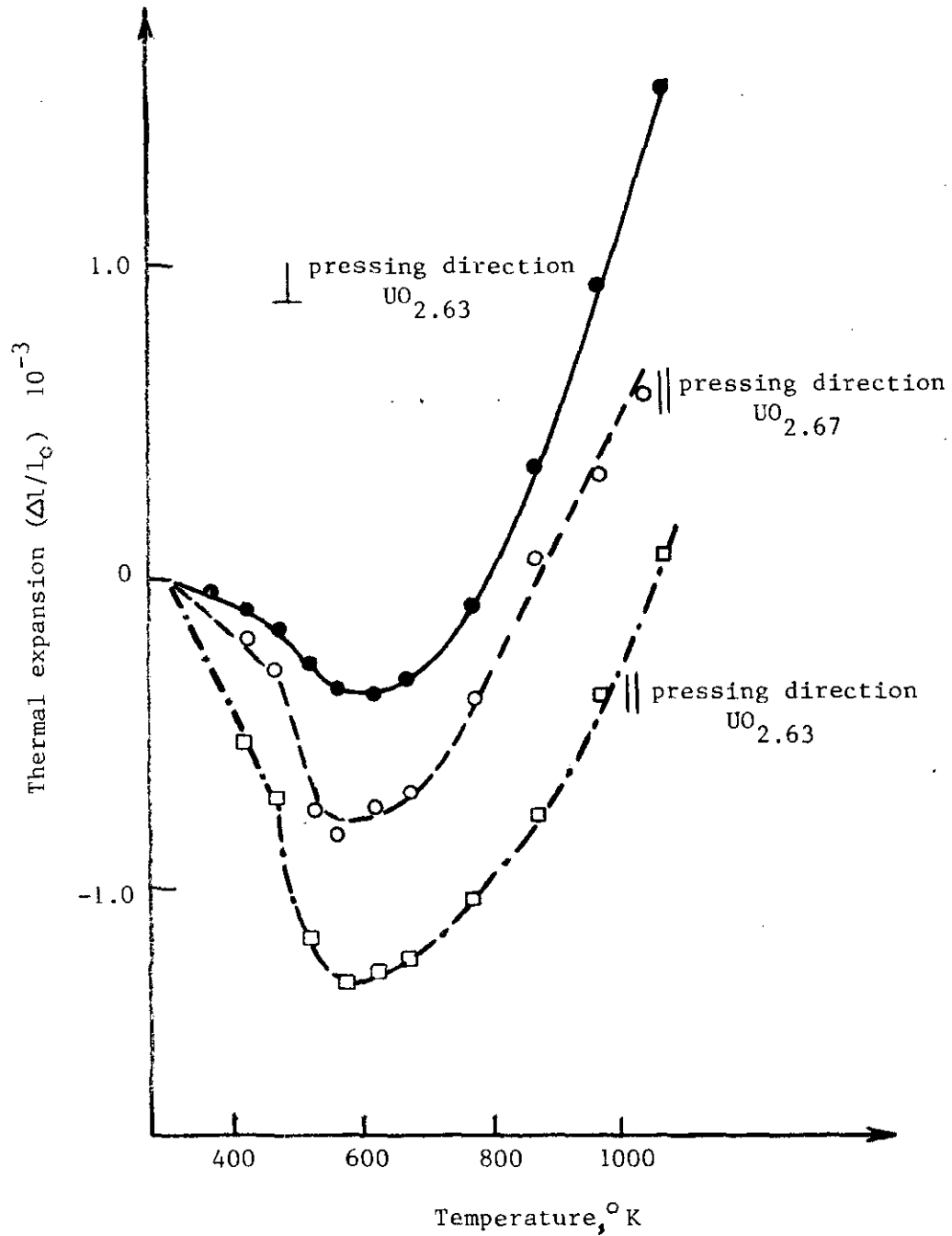


FIGURE 11. RELATIVE THERMAL EXPANSION OF $\text{UO}_{2.63}$ AND $\text{UO}_{2.67}$

Reference: Schulz, B., "Anomalie Der Thermischen Ausdehnung Und Wärmeleitfähigkeit Von U_3O_8 ," Rev. int. Htes Temp. et Refract. 12, pp 132-134, 1975

As the material is heated above 500°C during fabrication or irradiated in the reactor, there is a diffusion controlled reaction which occurs between the oxide and the aluminum matrix. This reaction produces phases according to the following proposed relationship.



This reaction will be discussed further in the section on Chemical Properties.

When the reaction occurs, the thermal expansion is expected to approach the expansion of UAl alloys⁽⁴⁰⁾.

2.6 Mechanical Properties

2.6.1 Unirradiated

2.6.1.1 Tensile and Elongation

Tensile tests were performed on sections cut from extruded fuel tubes containing 29 to 52 wt% U₃O₈ in aluminum. Cores were compacted from blends of commercial Alcoa 101 aluminum powder and U₃O₈ powder. The oxide powder contained the particle size distribution given in Table I for roll ground material. Each specimen was clad with 8001 aluminum alloy. Tests were done on a Baldwin tensile tester at a loading rate of 200 lbs/min.

Strength and elongation data are shown in Figures 12. The tensile strength of tube sections containing 30 wt% U₃O₈ is about 16 ksi. With increasing oxide content, the tensile and yield strengths decrease uniformly until about 46 wt% oxide. Around 46 wt% or 20 vol.%, the tensile strength suddenly decreases from about 12 ksi to about 7 ksi. Elongation at 30 wt% is 5.5% and decreases to 1.5% at about 50 wt%. Annealing the extruded tube specimens at 325°C for 1 hour decreased the tensile and yield strengths for a 46 wt% specimen by about 20% but increased the ductility by 4%.

The tensile strength of 8001 aluminum alloy (the cladding material) is about 19.5 ksi while the tensile strength for 1100 aluminum is 12.5 ksi at room temperature. The strength of Alcoa 101 is expected to be about the same as the 1100 alloy.

2.6.1.2 Bond Strength

The strength of the bond between the cladding and the core is determined for all SRS fuel elements. The bond strength is measured by welding two 3/8 inch diameter studs to each side of the cladding of a 1 inch square section cut from an extruded tube. The stud is resistance welded. The load needed to cause shear failure is determined by pulling the studs on a tensile tester.

Bond strength is shown in Figure 13 as a function of oxide content. Increasing the oxide loading causes the bond strength to continually decrease. At 18 wt% oxide, the bond strength is 17 ksi while at 66 wt% oxide it is 3 ksi. The strength approaches the shear strength of aluminum which is about 2 ksi.

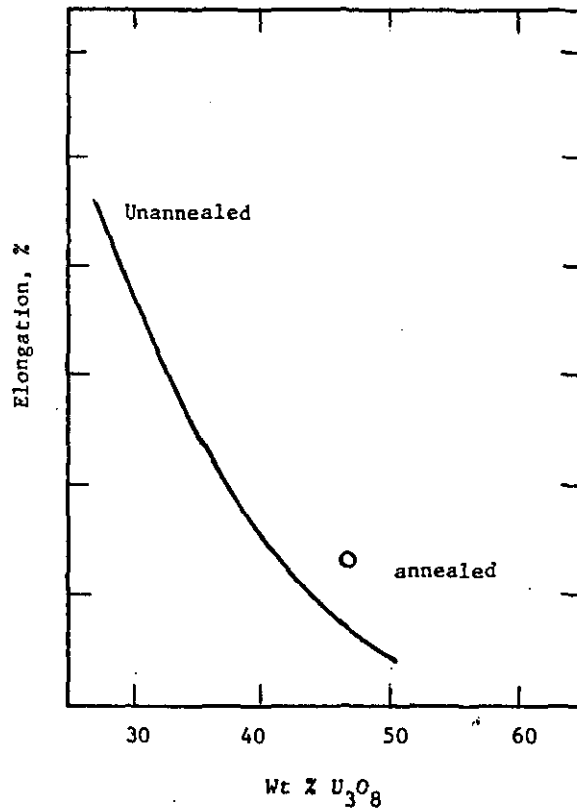
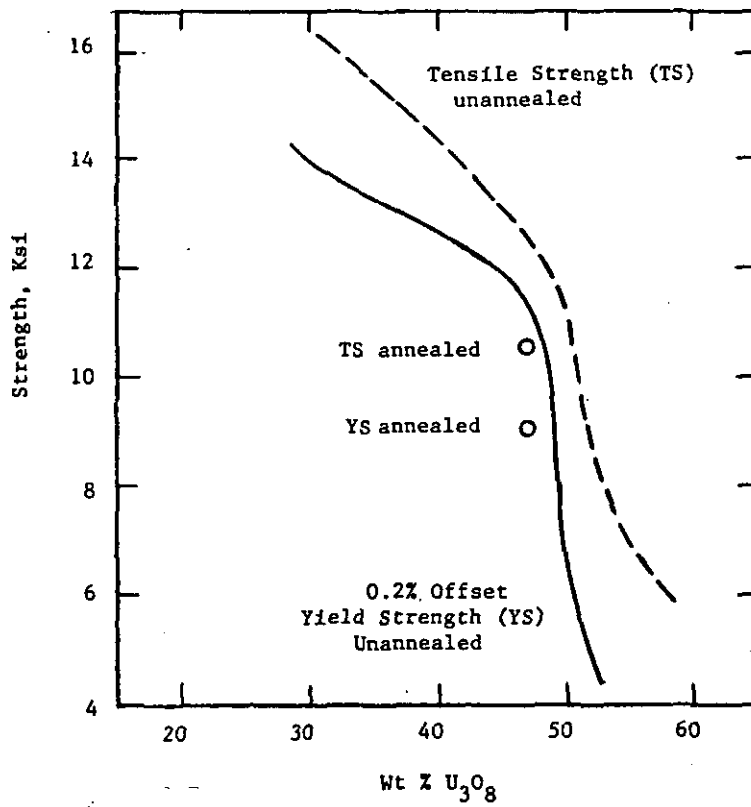


FIGURE 12. STRENGTH AND ELONGATION AT 25°C FOR EXTRUDED U_3O_8 -AL FUEL TUBES

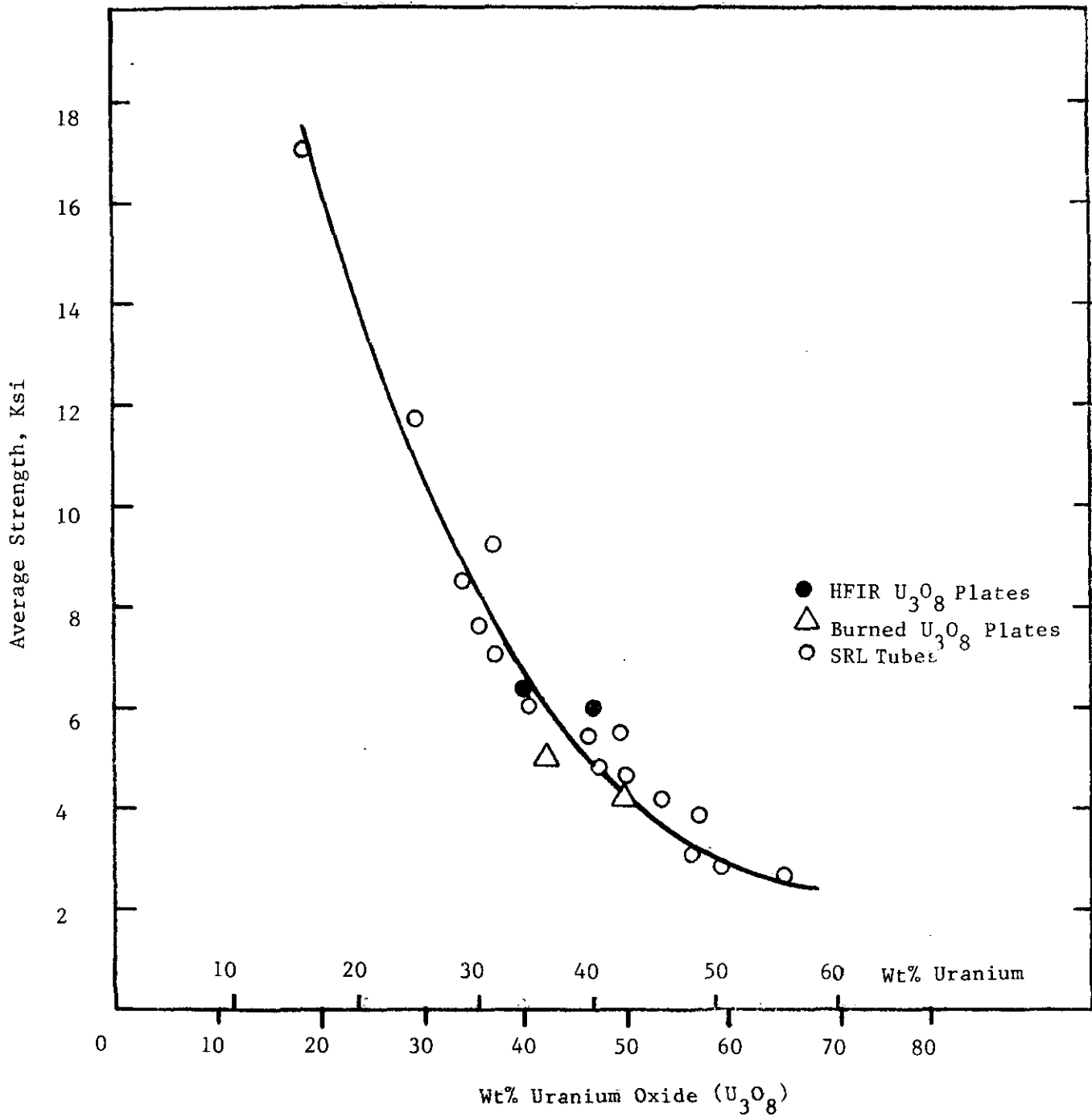


FIGURE 13. BOND STRENGTH FOR COEXTRUDED TUBES AND ROLLED FUEL PLATES

Also shown on the graph is the bond strength for the High Flux Isotope Reactor (HFIR) fuel plates from Oak Ridge. Plates containing both HFIR oxide and burned oxide were tested. Good agreement is found between the data for plate and extruded fuel elements.

2.6.2 High Temperature Strength

The strength necessary to collapse fuel tubes at and above the melting point of aluminum was determined for UAl alloy and U₃O₈-Al fuel tubes. The data is given in Table VI.

Three-inch sections were heated with a known weight placed on top of the section. The temperature at which the tube collapsed was recorded. The alloy section collapsed at about the melting point of aluminum (670°C) while the oxide PM section maintained its shape to higher temperatures. Without an applied stress, the tube section did not collapse until 1375°C. With a stress in the core of 11 psi, the section collapsed at about the melting point of aluminum (667°C). The strength above the aluminum melting point has been attributed to the aluminum oxide network developed in the core.

Due to the tube weight and vibration in the reactor, it is expected that the fuel would collapse as soon as the temperature of the tube reached 660°C or when the aluminum melted.

2.6.3 Irradiated

Mechanical properties have not been determined for irradiated cermet fuel elements. King, Long, Stiegler, and Farrell⁽⁴¹⁾ carried out tests for 8001 aluminum alloy which is used as the cladding material for SRS fuel elements. The studies were done to evaluate the microstructure and mechanical properties of as-irradiated and unirradiated 8001 aluminum. Annealing studies were also made to determine if irradiation damage could be annealed out.

Load-extension data are shown in Figure 14 for 8001 aluminum. Irradiation increased the strength and reduced the ductility by a factor of about 2.5 over unirradiated specimens. Irradiation to 1.0×10^{22} fast neutrons/cm² and over 10^{22} thermal neutrons/cm² caused the formation of approximately 10^{15} voids/cm³ whose diameters ranged up to about 550 Å. Irradiation hardening was decreased by testing at elevated temperatures or by annealing.

3.0 CHEMICAL PROPERTIES

Aluminum and uranium oxide mixtures are chemically reactive. The combination is unstable at temperatures above room temperature. Low temperature solid state reactions are classified as diffusion controlled reactions and occur below the melting point of aluminum, whereas high temperature exothermic reactions between liquid aluminum and oxide occur above the melting point of aluminum. For high temperature reactions, the fuel matrix is melted. This would occur only under severe accident conditions.

TABLE VI
AVERAGE AXIAL COMPRESSIVE STRESS AND TEMPERATURE TO COLLAPSE 53 WT% U₃O₈-AL AND 35 WT% U-AL OUTER TUBES IN AIR

Applied Load, lbs	Compressive Stress in the Core, psi	Collapse Temperature, °C	
		U ₃ O ₈ -Al	U-Al
0	-	1375*	670
1-1/2	2	917	-
3	4	915	-
6	7	669	-
8-1/2	11	667	-

*Collapsed when removed from furnace

Reference: Peacock, H. B., "Study of the U₃O₈-Al Thermite Reaction and Strength of Reactor Fuel Tubes," DP-1665

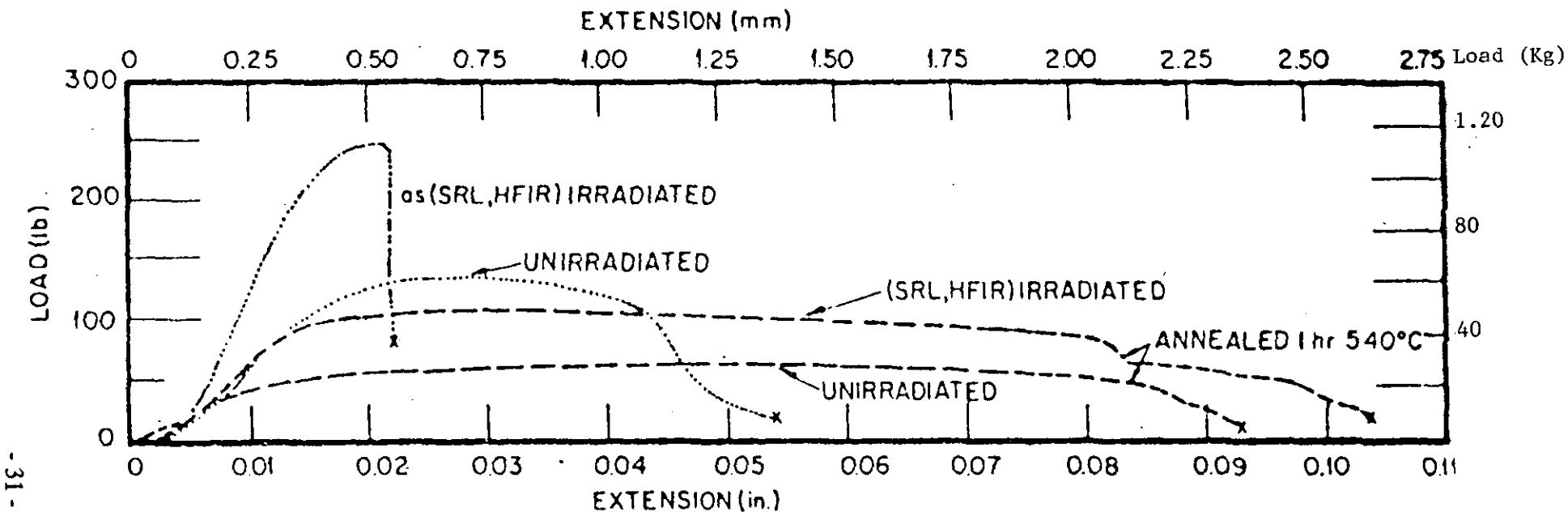


FIGURE 14. LOAD - EXTENSION DATA FOR UNIRRADIATED, IRRADIATED, AND ANNEALED 8001 ALUMINUM ALLOY

Reference: King, R. T., Long, E. L., Stiegler, J. O. and Farrell, K., "High-Neutron Fluence Damage in Aluminum Alloy," J. of Nuclear Materials, 35, pp. 231-243, 1970

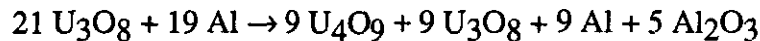
3.1 Low Temperature Reactions

When U_3O_8 and aluminum are heated at temperatures below the melting point of aluminum, a slow diffusion controlled reaction takes place. The percent reduction in U_3O_8 is shown in Figure 15 as a function of time at $600^\circ C$ for powders containing different amounts of fine particles (less than 44 microns). For an extruded tube section containing 28% fines, complete reaction would occur in about 45 hours at $600^\circ C$. The more fine particles the less time for complete reaction because of the increased aluminum-oxide surface area.

The reaction also depends on the calcining temperature of UO_3 used to form U_3O_8 . Reaction kinetics at $600^\circ C$ are faster for oxide calcined at $1400^\circ C$ than for oxide calcined at $800^\circ C$. U_3O_8 produced at the higher calcining temperature is more dense than the $800^\circ C$ material, thus enhancing the diffusion of uranium, oxygen, and aluminum.

3.1.1 Reaction Products

When U_3O_8 and aluminum tube sections are heated, uranium oxide is reduced to produce U_4O_9 (16). The reaction proposed is



Since this is diffusion controlled, a reaction layer of products is expected to exist around the U_3O_8 particles.

The effect of temperature on the reaction is shown in Figure 16 where the percent reduction to U_4O_9 is shown as a function of temperature at constant pressure and time(43). For a compacted mixture of U_3O_8 and aluminum, about 70% reduction occurred at $425^\circ C$. Almost complete conversion occurred at $525^\circ C$ in 24 hours.

To determine reaction time at $525^\circ C$, samples were heated for different times at constant temperature and pressure(43). The percent reduction is shown in Figure 17 as a function of time. The data indicate that the reduction of U_3O_8 by aluminum occurs fairly rapidly at $525^\circ C$ and 10^{-4} Torr. Reaction times greater than 10 hours are sufficient to cause complete reduction to U_4O_9 if the temperature is above $525^\circ C$.

Pressure does not normally affect solid state reactions but dissociation of U_3O_8 to U_4O_9 could occur, if the partial pressure of oxygen is low, according to the reaction



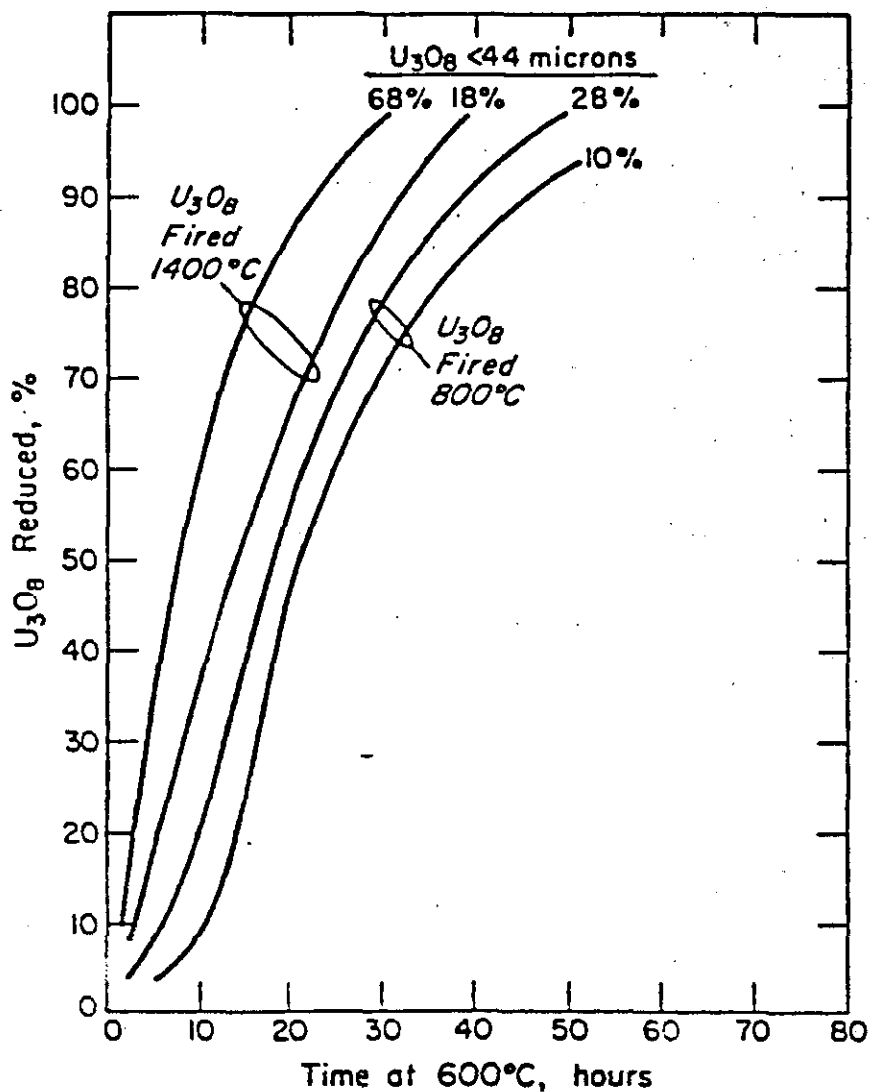


FIGURE 15. THERMAL REACTION IN SRS EXTRUDED AND UNIRRADIATED U_3O_8 -AL CERMET TUBE SECTIONS

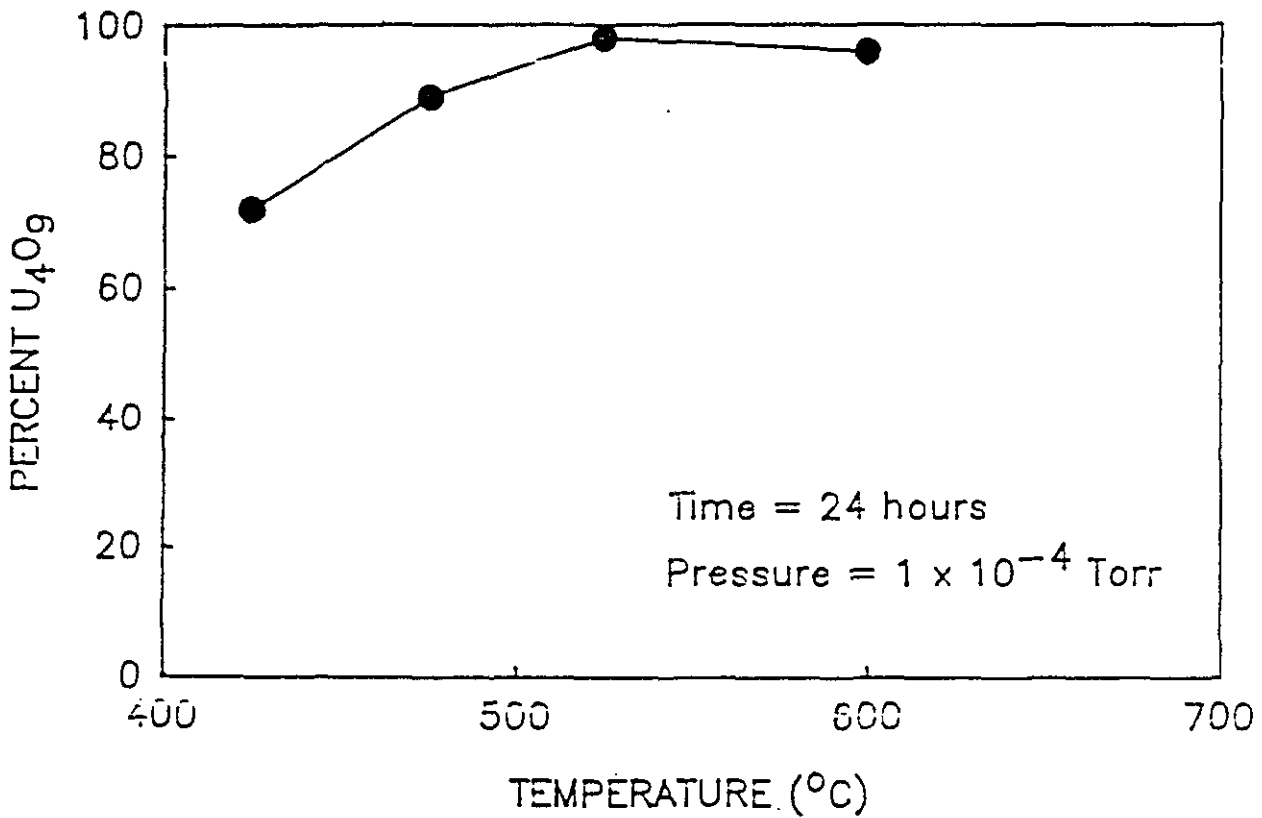


FIGURE 16. CONVERSION OF U₃O₈ TO U₄O₉ IN HEATED U₃O₈-Al PM COMPACTS AT DIFFERENT TEMPERATURES

Reference: Marra, J. E. and Peacock, H. B., "Reactions During the Processing of U₃O₈-Al Cermet Fuels," E. I. du Pont de Nemours and Company, DP-1776, June 1989

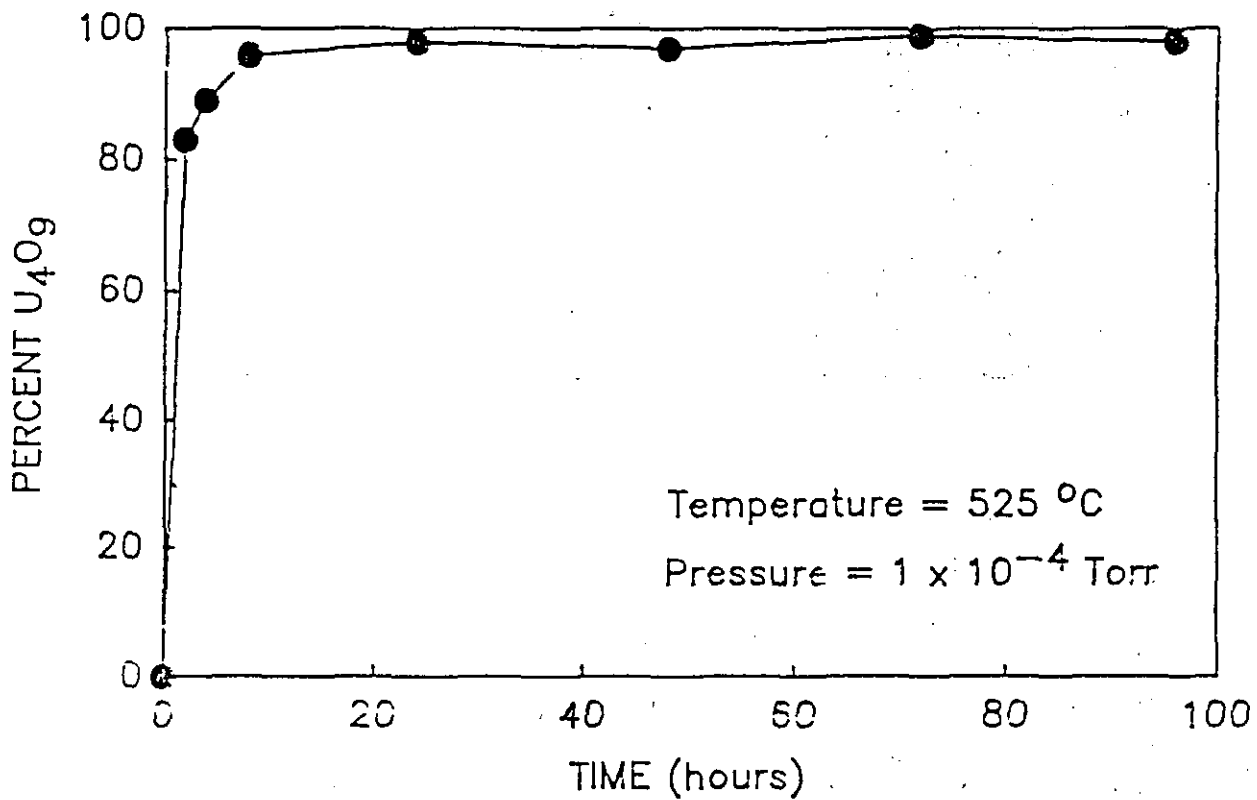


FIGURE 17. CONVERSION OF U₃O₈ TO U₄O₉ IN U₃O₈-Al PM COMPACTS WITH TIME AT CONSTANT TEMPERATURE AND PRESSURE

Reference: Marra, J. E. and Peacock, H. B., "Reactions During the Processing of U₃O₈-Al Cermet Fuels," E. I. du Pont de Nemours and Company, DP-1776, June 1989

Calculations indicate that for this to occur at 525°C the partial pressure of oxygen would have to be about 7×10^{-13} atmosphere. Samples were placed in evacuated ampules and heated at constant time and temperature to evaluate this effect. The lowest atmospheric pressure inside the ampules was approximately 10^{-6} Torr. Results are shown in Figure 18. There were difficulties in measuring the exact pressure inside the ampules. The lack of a clear pressure dependence implies that the reaction is most likely solid-state diffusion controlled.

A regression line drawn through the data indicates an increasing tendency for reduction with increasing ampule pressure. Griffith, Kim, and Froes⁽⁴²⁾ have shown that aluminum hydroxide on the surface of aluminum powder decomposes, releasing water which reacts with aluminum to release hydrogen. Hydrogen will reduce U_3O_8 to form U_4O_9 . This could be an explanation of the effect observed because the moisture content is expected to be greater at higher pressures.

The degree of reaction for a compacted sample was determined at different stages of manufacture. X-ray diffraction was used to detect the presence of U_4O_9 . The results are shown in Tables VII and VIII. From the data, it is expected that over 50% reduction of the oxide to U_4O_9 takes place. The fuel in fabricated tubes consists of equal amounts of U_3O_8 and U_4O_9 . Samples were taken through the 1 inch thick compacted core to determine if the reduction was uniform. The ratio of U_4O_9/Al is shown in Table VII. The almost constant ratio indicates uniform reduction.

3.2 Exothermic Reactions

At temperatures above the melting point of aluminum, an exothermic reaction can take place between uranium oxide and molten aluminum. The reaction theoretically releases about 225 kcal per gm of U_3O_8 . Many studies have been done to evaluate the consequence of the reaction on reactor operation in case of an accident^(43, 44, 45, 46). It has been the conclusion of most investigators that if it occurred, practically no additional effects would result from the released energy.

The amount of energy released for U_3O_8 and aluminum was calculated by Fleming and Johnson⁽⁴⁵⁾ and is shown in Figure 19. The result is based on the maximum credible energy released by assuming a stoichiometry productive of the greatest energy evolution. The maximum energy release, according to the calculation, should occur at about 60 wt% U_3O_8 in aluminum. Experimental data obtained by Fleming and Johnson were too few and scattered to provide statistical support for the calculation. However, results did show an ignition temperature for the reaction to range between 815 and 1049°C and a maximum temperature $>2200^\circ C$ at the surface of a compacted pellet.

At SRL, compacted pellets containing 53 wt% oxide with different particle-size distributions of U_3O_8 in commercial Alcoa 101 aluminum powder were heated in a furnace in air⁽⁴⁵⁾. Thermocouples recorded the temperature-time response. Response curves for compacted pellets are shown in Figure 20. In Figure 21, the response curve for an extruded tube section containing roll ground particle-size distribution of oxide is compared with a pellet containing a similar particle-size distribution.

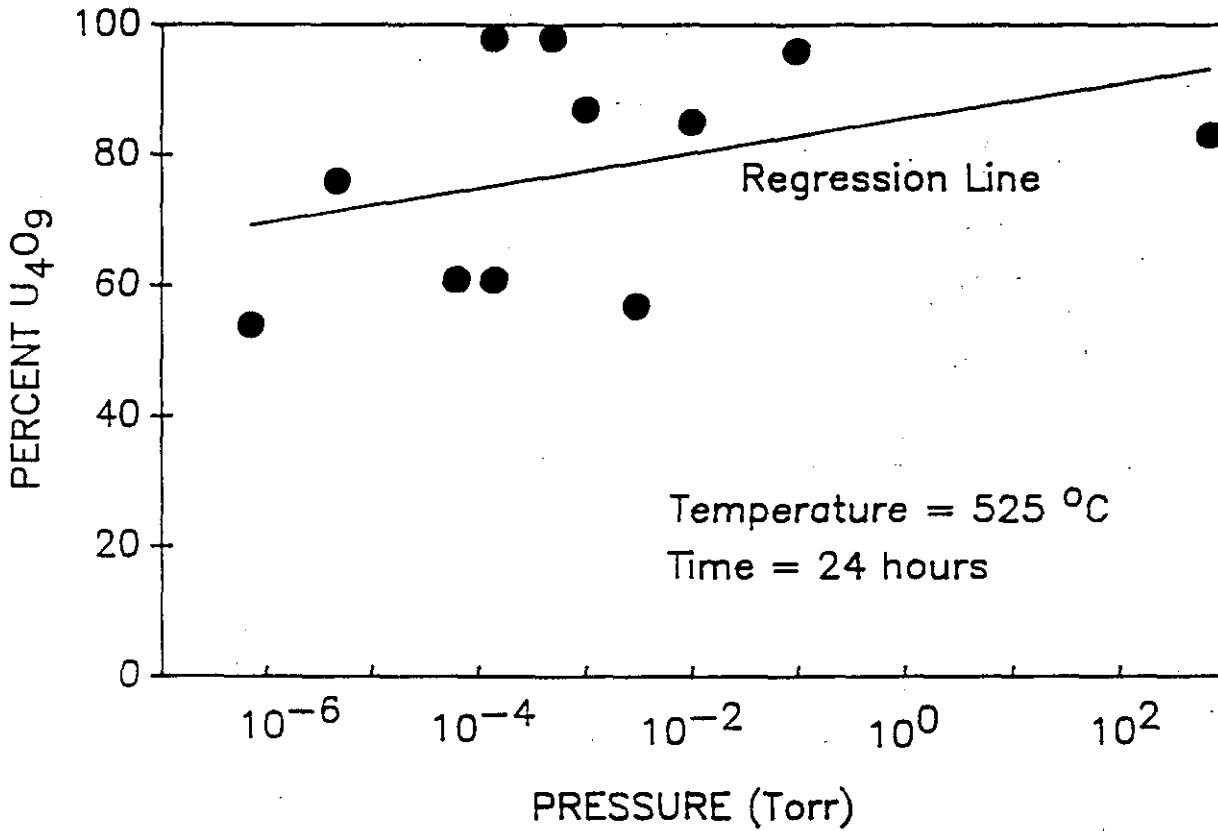


FIGURE 18. EFFECT OF PRESSURE ON U₃O₈ TO U₄O₉ CONVERSION REACTION

Reference: Marra, J. E. and Peacock, H. B., "Reactions During the Processing of U₃O₈-Al Cermets Fuels," E. I. du Pont de Nemours and Company, DP-1776, June 1989

TABLE VII
PHASE ASSEMBLAGE DETERMINED AFTER VARIOUS STAGES OF
THE POWDER METALLURGY PROCESS

Sample	Relative Oxide Content in Core	
	U ₃ O ₈	U ₄ O ₉
Feed Powder	100%	0%
As-Compacted	100%	0%
Vacuum Degassed at 525°C	42%	58%
Extruded	58%	42%

TABLE VIII
EFFECT OF CORE POSITION ON THE U₄O₉ CONTENT
OF VACUUM DEGASSED SAMPLE

Position	U ₄ O ₉ /Al Ratio
Outside	0.432
Center	0.424
Inside	0.439

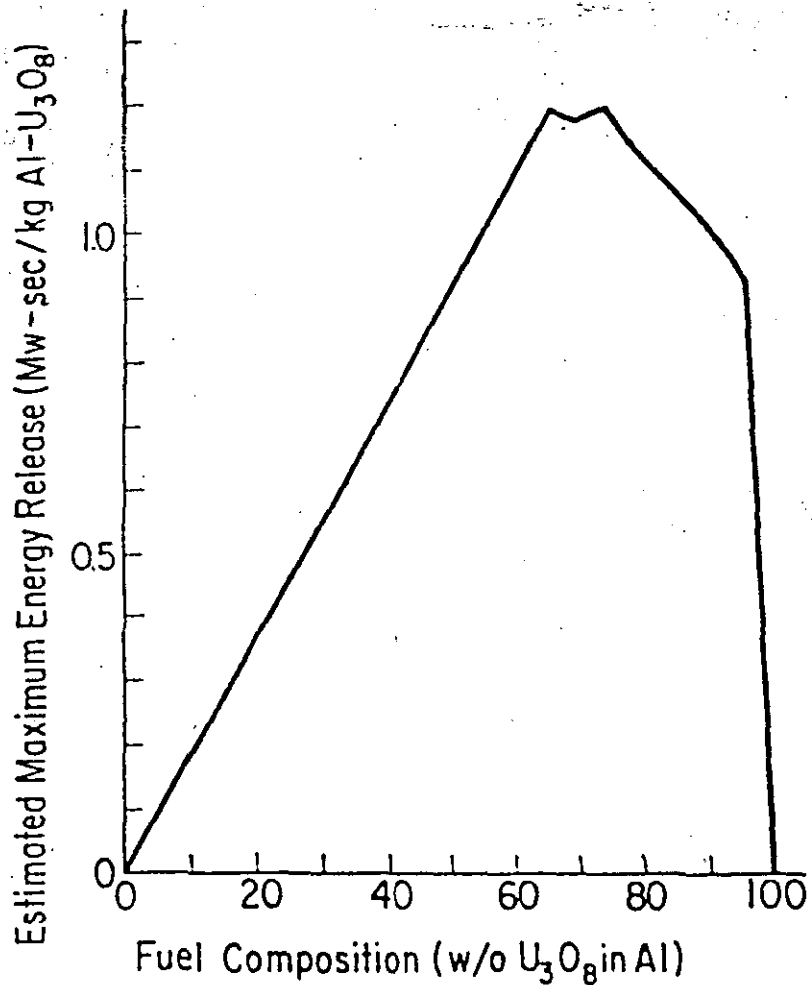


FIGURE 19. ENERGY RELEASE AS A FUNCTION OF FUEL COMPOSITION FOR U₃O₈-Al METALLOTHERMIC REACTION

Reference: Fleming, J. D. and Johnson, J. W., "Aluminum-U₃O₈ Exothermic Reactions, Nucleonics," Vol. 21, No. 5, May 1963

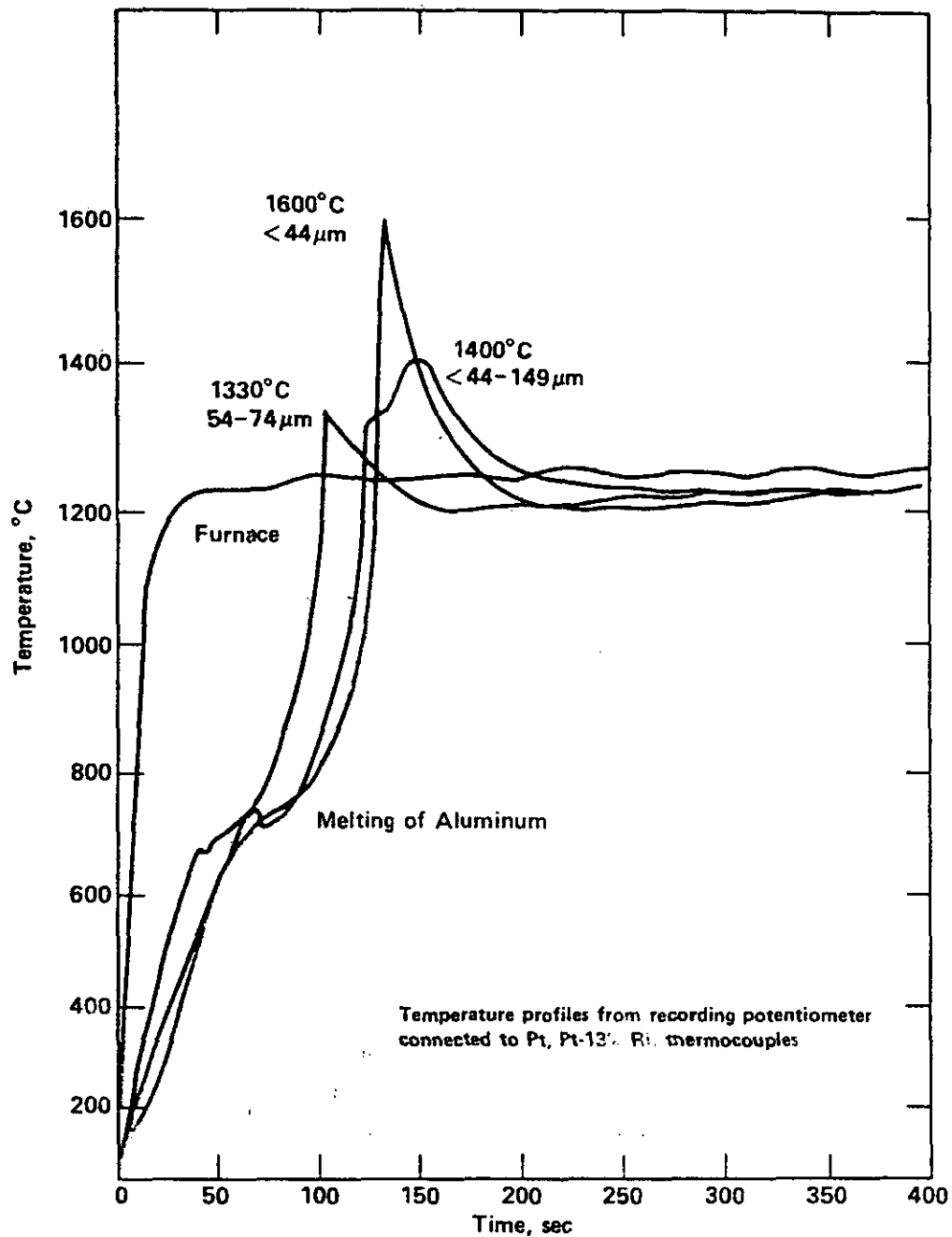


FIGURE 20. EFFECT OF U_3O_8 PARTICLE SIZE ON THERMAL REACTIONS IN RAPIDLY HEATED 53 WT % U_3O_8 -Al PELLETS

Reference: Peacock, H. B., "Study of the U_3O_8 -Al Thermite Reaction and Strength of Reactor Fuel Tubes," E. I. du Pont de Nemours and Company, DP-1665, August 1983

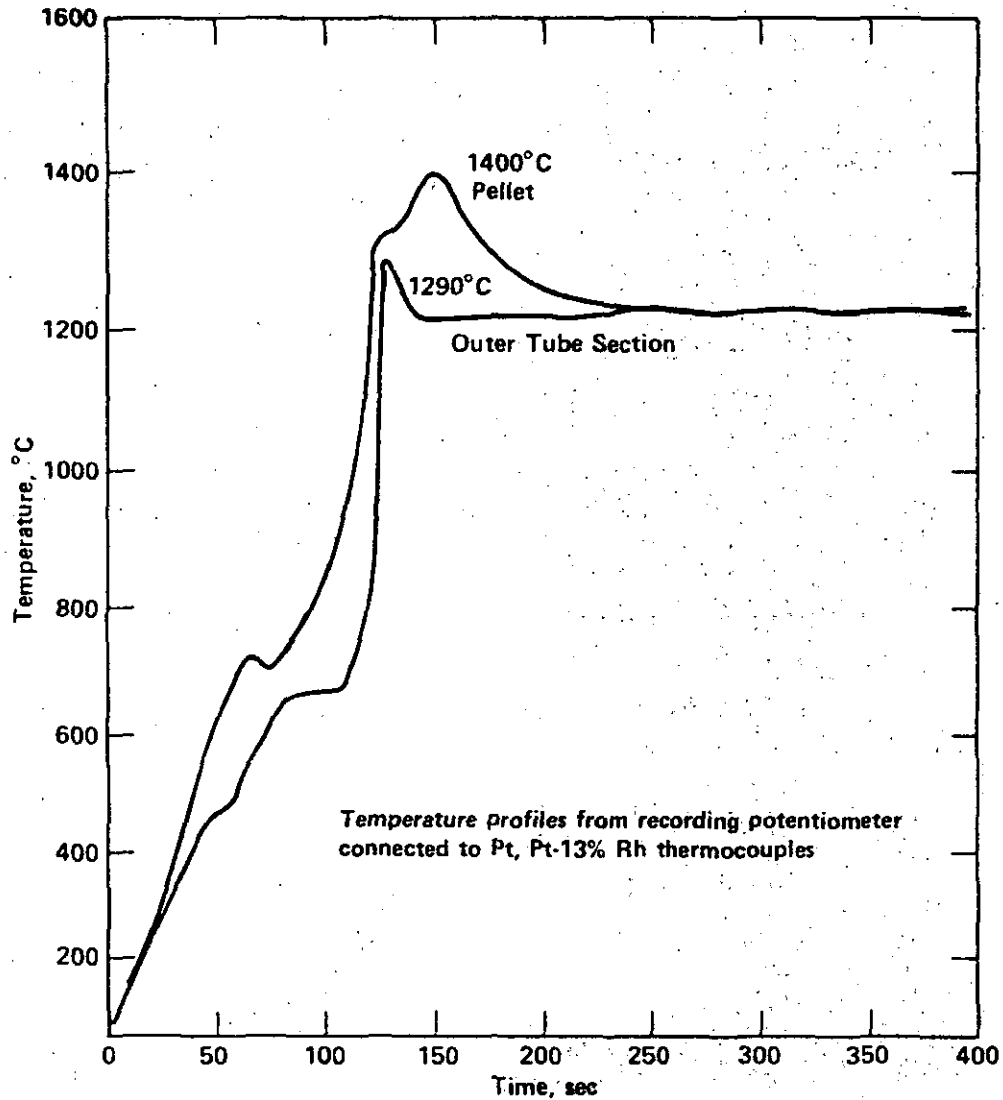


FIGURE 21. COMPARISON BETWEEN TIME-TEMPERATURE CURVES FOR A 53 WT % U_3O_8 -Al PELLET AND AN OUTER TUBE SECTION PLUNGED INTO A PREHEATED FURNACE

Reference: Peacock, H. B., "Study of the U_3O_8 -Al Thermite Reaction and Strength of Reactor Fuel Tubes," E. I. du Pont de Nemours and Company, DP-1665, August 1983

The data indicated that the exothermic reaction occurred above 900°C, well above the melting point of aluminum. It was also a function of particle size distribution of the oxide with fine powder, producing lower ignition temperature and the highest peak temperature. The tube section had the lower peak temperature of 1290°C.

Pasto, Copeland, and Martin⁽⁴⁶⁾ studied the U₃O₈-Al exothermic reaction for the Reduced Enrichment for Research and Test Reactor program. The specimens tested were punched from simulated fuel plates of two different compositions and similarly yielded ΔH results lower than expected. The following is a summary from their report:

On heating, U₃O₈-Al mixtures of 50 wt% and 79 wt% oxide exhibited several distinct thermal energy releases or absorptions. These include an exotherm between 600°C and the melting point of aluminum, an endotherm on melting of aluminum, an exotherm at near 900°C, and one or two more exotherms at > 1200°C..

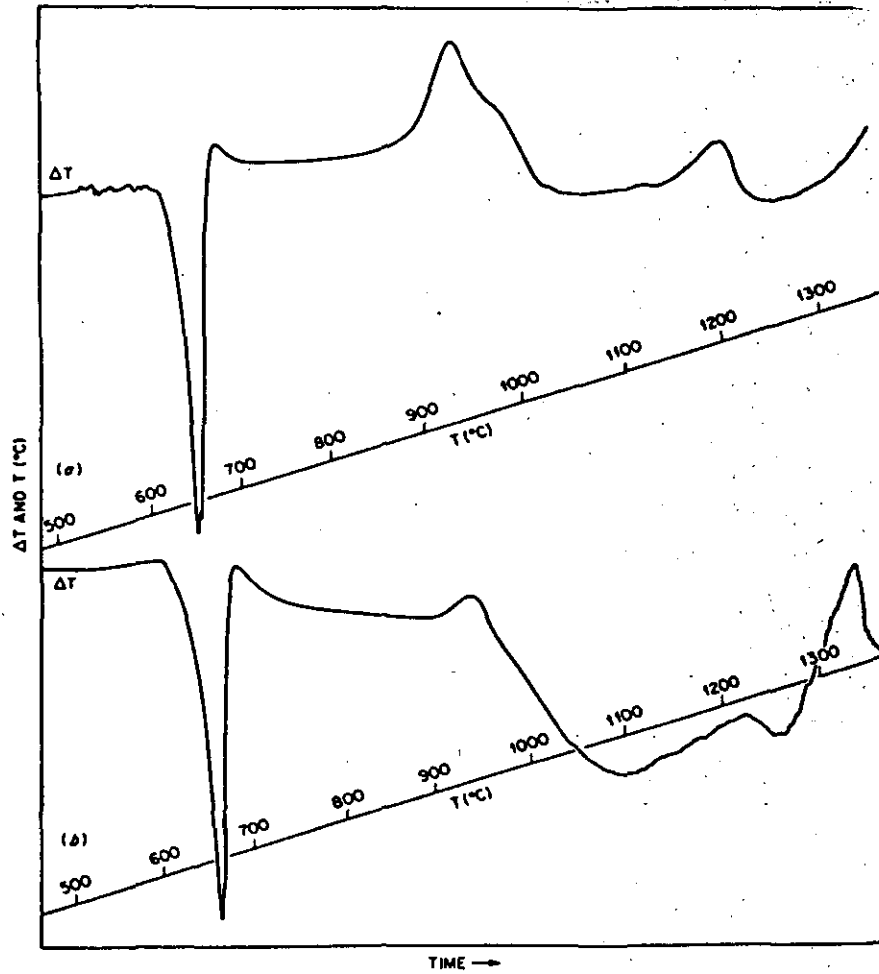
Quantitative analysis of the areas encompassed within these exo- and endotherms yields good accuracy (<10% error) for values of the heats of transformation.

Using the quantitative analysis technique, heats of the three U₃O₈-Al compositions were calculated. These results were all much lower than values described in the literature, based on thermochemical considerations.

Figure 22 is from the ORNL work.⁽⁴⁶⁾ It shows a clearly defined exothermic peak at around 950°C which is much lower in magnitude than had been reported in earlier literature. The ORNL equipment was not calibrated at the 1200 to 1350°C temperatures of the next exothermic peak and thus the energy level of this peak could not be quantified. There was no explanation for the upper peak from the ORNL data; however, from the more recent SRS results discussed below, it is clearly due to partial conversion of the U₃O₈ to U₄O₉ during the fabrication process. The peak at about 950°C is from the U₄O₉ and the higher temperature peak is from the remaining U₃O₈.

The fuel plate containing 75 wt% U₃O₈-25 wt% Al was heated to 1400°C. This composition is expected to exhibit maximal energy release on reaction. No ill effects other than warping was observed. The results indicated that the heat evolved from the thermite reaction in this type fuel plate was not likely to pose any safety problems in the reactor.

Recent studies at SRL have shown that the ignition or onset reaction temperature for a mixture of U₃O₈/U₄O₉ is a function of the percent U₄O₉ in the mixture. U₄O₉ has an onset temperature of about 850-900°C, and U₃O₈ has an ignition temperature of about 1200°C. By varying the ratio of the two components, the ignition temperature increases according to Figure 23. This could explain the several exothermic reaction peaks observed above the melting point of aluminum.



**THERMITE REACTION HEATS
(J/g FUEL)**

TOTAL Al CONTENT (wt %)	THERMITE REACTION HEATS (J/g FUEL)	
	MEASURED	LITERATURE
52-56	243	830-900
63-67	71	650-710

FIGURE 22. ORNL DTA STUDY OF U₃O₈-Al METALLOTHERMIC REACTION

Reference: Pasto, A. E., Copeland, G. L. and Martin, M. M., "Quantative Differential Thermal Analysis Study of the U₃O₈-Al Thermite Reaction," Bull of the Am Ceramics Soc., 61, p 491, 1982

It is postulated that the formation of reaction products occurs by diffusion of uranium and aluminum to the outer boundaries of the U_3O_8 particles. If a mixture is heated slowly, then reactions could proceed and thus eliminate the exothermic reaction above $900^\circ C$.

An extruded tube section was heated at $21^\circ C/min$ in a furnace in air. The temperature-time response was recorded and is shown in Figure 24. Aluminum melted at approximately $660^\circ C$ and no indication of an exothermic reaction occurred until about 850 to $900^\circ C$. The energy release was minor indicating a small reaction took place. It is expected that a diffusion controlled reaction occurred as the material was slowly heated. The reaction products were UAl_x and Al_2O_3 and some residual U_4O_9 . At 850 - $900^\circ C$, the remaining U_4O_9 reacted.

4.0 IRRADIATION PERFORMANCE

Enriched uranium oxide fuel has been used in several reactors in the US and abroad. Irradiation performance has been satisfactory with no known accidents associated with its use. The U_3O_8 -Aluminum fuel has been evaluated and tested for possible use in The Savannah River Production Reactors as extruded tubes.

4.1 Irradiation Conditions

Irradiation conditions for tests conducted at Savannah River using Mark 14 geometry fuel tubes are given in Table IX. Extruded tubes containing approximately 18 to 59 wt% oxide have been successfully irradiated to fission densities up to 1.6×10^{21} fissions per cc of core. The higher loadings stayed in the reactor up to 208 days before being removed for inspection and evaluation.

4.2 Microstructure

Photographs of irradiated fuel tube sections are shown in Figure 25. As the exposure, temperature, and time increased, the amount of reaction observed between the U_3O_8 particles and aluminum increased. The reaction products expected but not confirmed are UO_2 , U_4O_9 , UAl_x , and Al_2O_3 .

There were some particles within the fuel matrix which contained what appeared to be oxide with reaction products formed around the outer boundary of the particle. This was particularly true for low weight percent cores which experienced low temperature during irradiation. Cores containing 59 wt% oxide have very little residual aluminum and only a few oxide containing particles. At approximately 64 wt% U_3O_8 , stoichiometric calculations indicate that no residual aluminum is left in the core after forming UAl_4 and Al_2O_3 .

The kinetics for the oxide-aluminum reaction in the reactor is not known but it is expected to be much faster than outside the reactor because of irradiation enhanced diffusion and steep temperature gradients near fuel particles.

Microstructural changes that occurred during irradiation of enriched burned and high-fired (HFIR) U_3O_8 dispersions in fuel plates were reported by Martin, Richt, and Martin⁽⁴⁷⁾. Both fuel types reacted with the aluminum matrix but the extent of the reaction was greater for the burned U_3O_8 dispersions. This material was calcined at $800^\circ C$ instead of $1400^\circ C$ for the HFIR U_3O_8 .

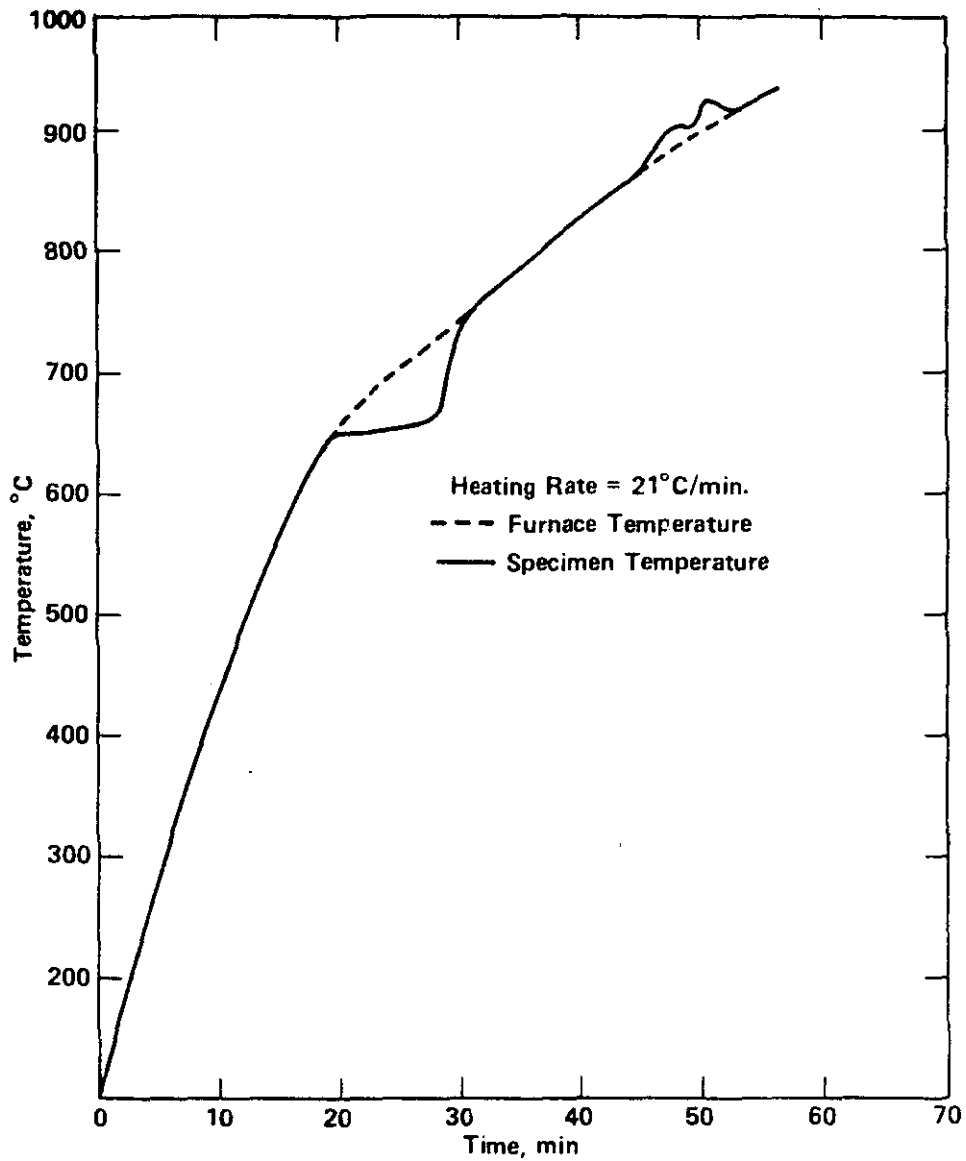


FIGURE 24. TEMPERATURE OF SLOWLY HEATED OUTER TUBE SECTION WITH A 53 WT % U_3O_8 -Al CORE

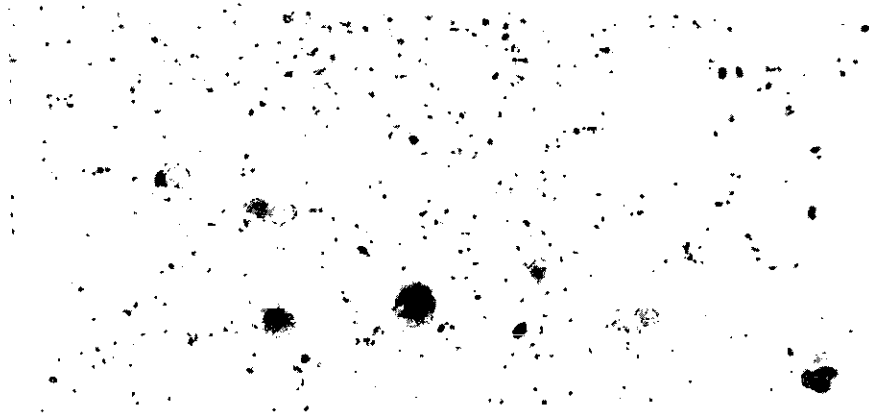
Reference: Peacock, H. B., "Study of the U_3O_8 -Al Thermite Reaction and Strength of Reactor Fuel Tubes," E. I. du Pont de Nemours and Company, DP-1665, August 1983

TABLE IX
SRL IRRADIATION TEST OF P/M FUEL TUBES

Number Irradiated ^b	U	Wt %		Average Fission Density ($10^{21}/\text{cc}$ Core)	Max Core Temp ^a , °C	Irradiation, days
		U ₃ O ₈	Fines (<325 Mesh)			
5	12	17.6	68	0.5	195	105
4	25	29.5	68	0.7	200	122
15	33-50	38-59	40	1.0	220	140-208

a. Calculated using predicted aluminum oxide thickness and measured hot spot factor.

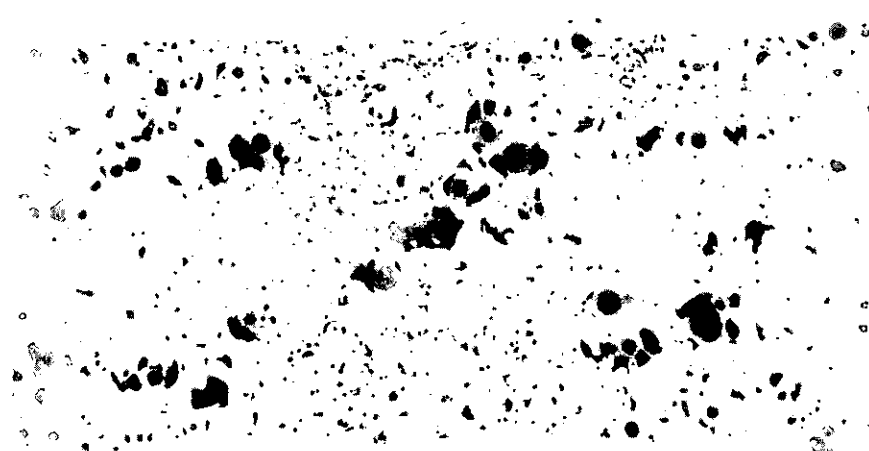
b. Mark 14 geometry; 0.040 inch thick core with 0.020 inch aluminum cladding.



a) 18 wt% U_3O_8 in Aluminum, 5×10^{20} Fissions/cc core. 50X



b) 38 wt% U_3O_8 in Aluminum, 1.6×10^{21} Fissions/cc core, 50X



c) 59 wt% U_3O_8 in Aluminum, 1.6×10^{21} Fissions/cc core, 50X

FIGURE 25. PHOTOMICROGRAPH OF IRRADIATED U_3O_8 -ALUMINUM TUBE SECTIONS

X-ray diffraction techniques were unsuccessful for phase identification in irradiated fuel. Only peaks corresponding to the aluminum matrix were observed. Uranium and fission product peaks were absent because of irradiation damage to the structure.

Less extensive reactions occurred at lower irradiation temperatures which was consistent with earlier data⁽⁴⁸⁾.

The effect of irradiation temperature on the extent of the reaction is shown in Figure 26. As the nominal cladding temperature increased, the extent of the reaction increased giving a lower volume fraction of aluminum in the core. Martin et al concluded that the extent of the reaction was primarily a function of the irradiation temperature and not burnup.

Electron-microprobe analysis on one of the irradiated HFIR dispersions indicated that at least some of the reaction phases between U_3O_8 and aluminum were present. The relative uranium and aluminum distribution across a typical U_3O_8 fuel particle is shown in Figure 27. No attempt was made to define the phases present from microprobe data.

Hofman, Copeland, and Sanecki⁽⁴⁹⁾ suggested that during irradiation a somewhat different reaction from that reported in the out-of-pile studies actually takes place, a reaction by which the interior of the U_3O_8 particles is reduced to UO_2 in order to supply the U_3O_8 -Al reaction front with oxygen.

4.3 Swelling and Blister Threshold Temperature

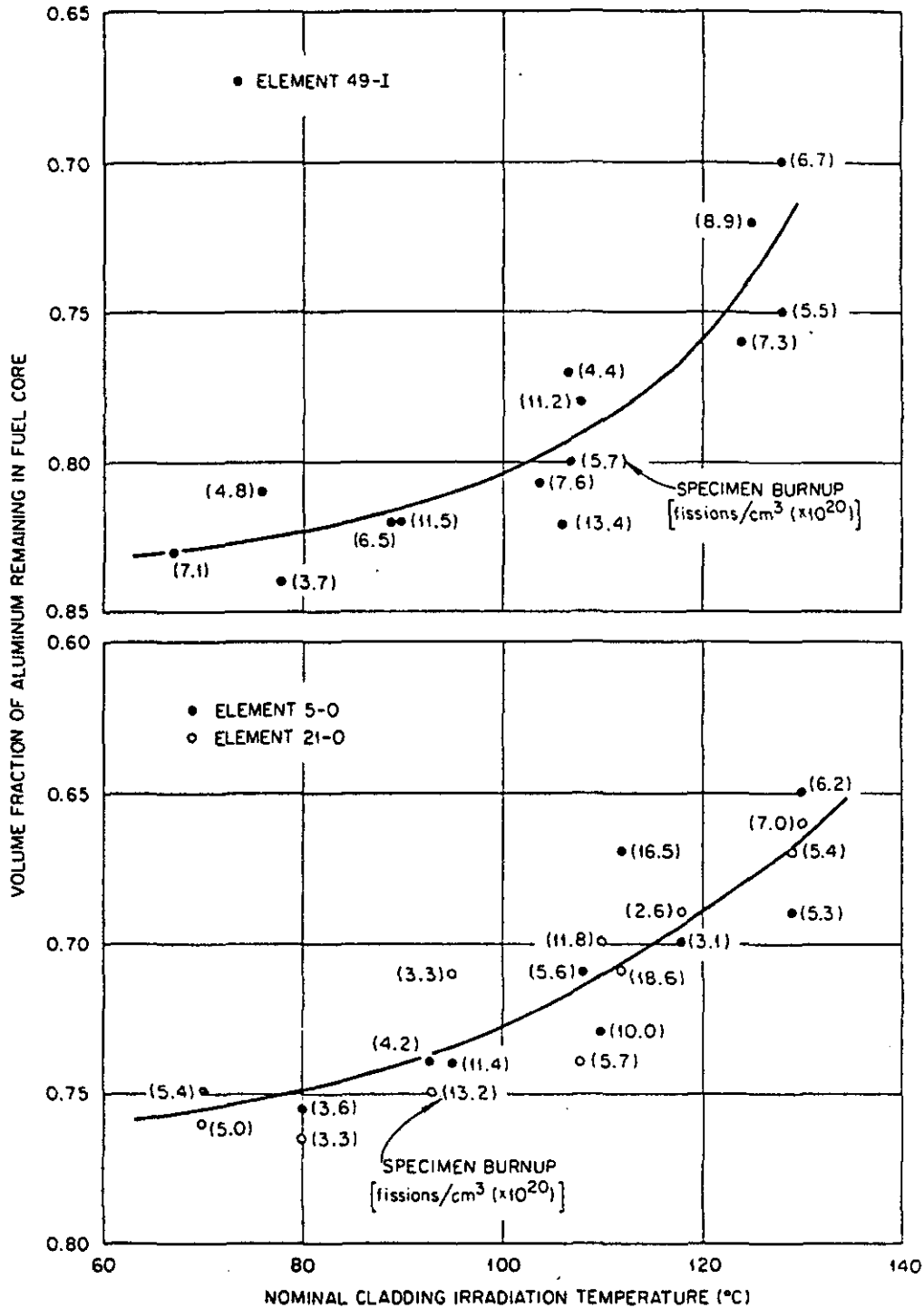
Uniform swelling or increase in volume of a cermet fuel element occurs primarily because of fission gas pressure within the elements. The solid-state, diffusion reaction between oxide and aluminum produces a negative volume change and would not contribute to swelling behavior. Blistering is the formation of localized bubbles on the fuel element surface. The bubbles result from increased gas pressure during heating of the irradiated plate or tube section. Each phenomena will be discussed separately for oxide tubes.

4.3.1 Swelling

Fission gases generated during irradiation are accommodated within fuel particles or within voids. Extruded cermet fuel tubes contain a large fraction of particle and fabrication voids as indicated in Figure 7 of this report. Fabrication voids, which are due to metal working operations, increase with increasing oxide content. Swelling of fuel tubes is expected to decrease with increasing oxide content. This has been observed for miniature fuel plates⁽⁴⁷⁾.

The uniformity of swelling of SRS irradiated fuel tubes was determined by measuring the thickness of tube sections using a fixture having a dial indicator.

ORNL-DWG 71-5805



FIG

FIGURE 26. EFFECT OF IRRADIATION TEMPERATURE UPON THE EXTENT OF REACTION IN THE CORES OF THE INNER (TOP) AND OUTER (BOTTOM) ANNULUS HFIR FUEL PLATES

Reference: Richt, A. E., Knight, R. W., and Adamson, Jr., G. M., "Pastirradiation Examination and Evaluation of the Performance of HFIR Fuel Elements," Oak Ridge National Laboratory, ORNL-4714, December 1971

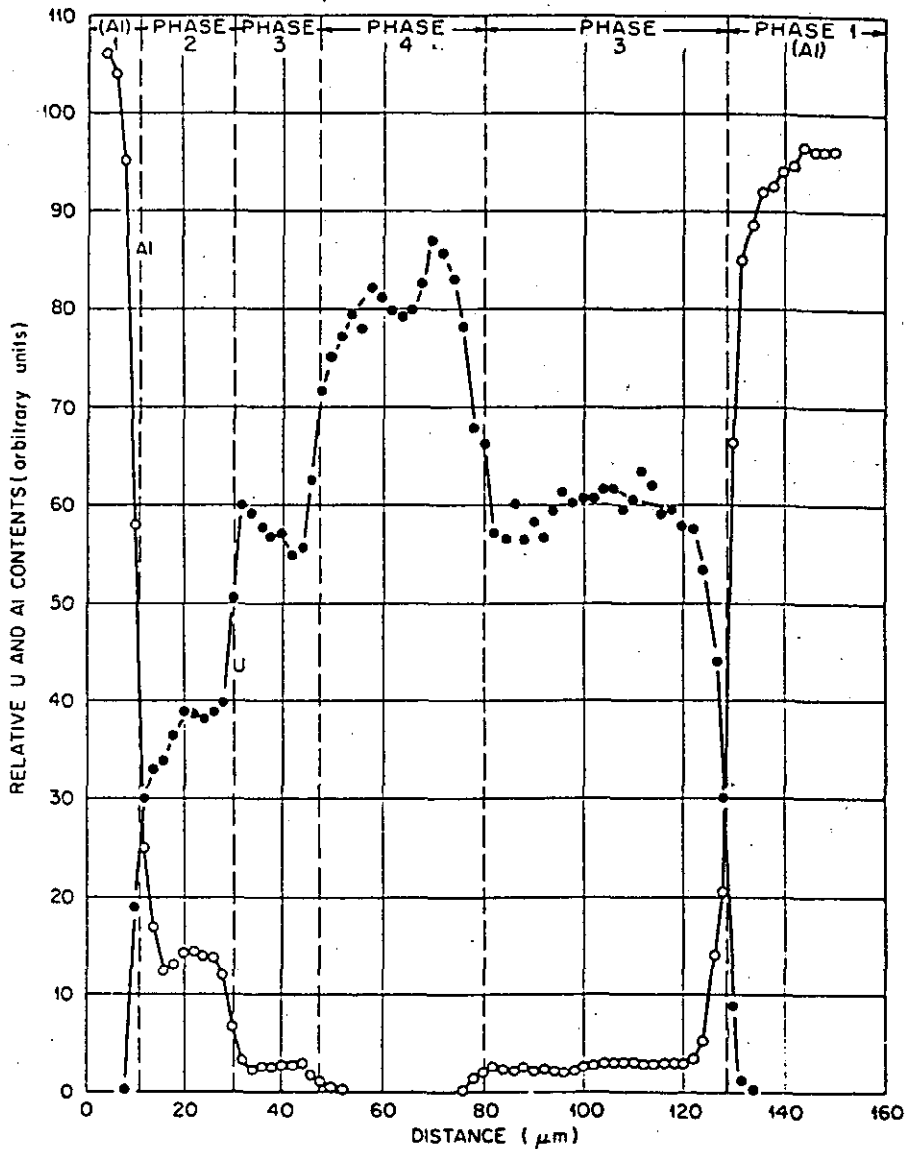
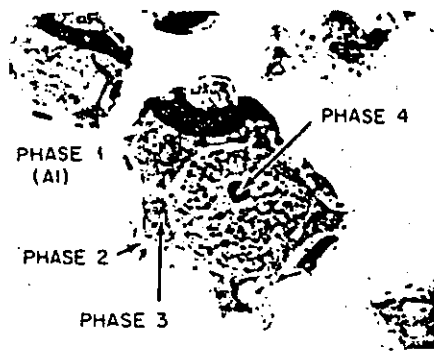


FIGURE 27. RELATIVE URANIUM AND ALUMINUM DISTRIBUTION ACROSS A TYPICAL FUEL PARTICLE OF AN IRRADIATED U₃O₈ FUEL DISPERSION

Reference: Martin, M. M., Richt, A. E., and Martin, W. R., "Irradiation Behavior of Aluminum-Base Fuel Dispersions," Oak Ridge National Laboratory, ORNL-4856, May 1973

Results from measurements of as-extruded fuel elements are presented in Table X. Measurements were made at four positions around the circumference of the tubes. These values were averaged because during extrusion sometimes the outside and inside diameters are eccentric. The average wall thickness for extruded tubes was about 79 mils (0.079 inches). Process specification for the wall thickness of extruded tubes was 80 ± 5 mils.

During irradiation, there is a buildup of oxide on the outer and inner surfaces of the tube. The oxide thickness amounts to about 1 mil on each surface. Adding the oxide thickness of the average tube thickness for the fabricated tube gives an expected value of about 81 mils for an irradiated tube.

Data is shown in Tables XI and XII for tube wall thickness of cermet tubes containing about 18 and 30 wt% U_3O_8 and irradiated to 5×10^{20} and 7×10^{20} fissions/cc of core, respectively. Practically no swelling was observed when wall thickness values obtained from the extruded tubes are compared with the measured values of irradiated tubes. For these tubes, the average void content was 3 and 8 % before irradiation, respectively. Measurements made from the photographs in Figure 25 indicate that the core swelled approximately 5% at a fission density of 1×10^{21} .

4.3.2 Blistering

An annealing test is normally used to determine the threshold temperature for blister formation. About 3-inch long sections from irradiated tubes were cut and heated at temperature for one hour. If blisters did not form on the surface, then the temperature was increased.

The possible blistering region for U_3O_8 -Aluminum tubes is shown in Figure 28 as a function of exposure in fission/cc of U_3O_8 . Oxide was produced by calcining at either 800°C or 1400°C. The blister resistance appeared to be somewhat higher for the low temperature calcined oxide. The reason could be that oxide calcined at the higher temperature sintered the material and reduced particle porosity. Porosity can contain fission gas during irradiation.

The data shows a particle size effect. At 7.1×10^{21} fissions/cc of U_3O_8 , tubes containing low wt% fine particles (< 44 microns) have a higher blister temperature. This effect maybe associated with fission recoil. A larger fraction of fission gases tends to escape from smaller oxide particles.

The blister temperature ranged from about 400°C to 600°C. At highest oxide loading and exposure, the blister temperature was 600°C for tubes containing oxide calcined at 800°C with 40% fines.

Photographs of tube section that were blister tested are shown in Figure 29. Sections have been heated to 600°C without exothermic reactions taking place.

TABLE X
TYPICAL WALL THICKNESS MEASUREMENTS
FOR AS-EXTRUDED U₃O₈-Al TUBES (MK 14)

Tube #	THICKNESS, MILS				Tube Average
	0°	90°	180°	270°	
14-50	78.0	78.0	78.0	78.0	78.0
14-26	78.5	78.5	79.0	79.0	78.8
14-20	77.0	79	82.0	80.5	79.6
14-51	77.5	79.0	80.0	78.0	78.6
14-28	78.5	79.5	80.0	79.0	79.3
				Average	78.9

* Average of measurements made on front and rear of the tube. (Process specification of 80 mils, as fabricated)

TABLE XI
THICKNESS MEASUREMENTS FOR TUBES
IRRADIATED TO 5×10^{20} FISSIONS/CC CORE

Tube #	THICKNESS, MILS				Tube Average
	0°	90°	180°	270°	
14-21	82.9	81.7	81.8	81.5	82.0
14-24	83.2	82.6	81.1	81.0	82.0
14-27*	84.6	82.9	78.6	81.9	82.0

* Tube contained HFIR U₃O₈

TABLE XII
THICKNESS MEASUREMENTS FOR TUBES
IRRADIATED TO 7×10^{20} FISSIONS/CC CORE

Tube #	THICKNESS, MILS				Tube Average
	0°	90°	180°	270°	
14-21	81.0	82.0	88.0	83.0	83.5
14-23	87.5	82.5	83.5	85.5	84.5
14-24	82.5	80.5	83.0	84.5	82.6
14-27*	86.0	83.0	80.0	81.0	82.5
14-30	81.0	81.0	82.0	83.0	81.8
14-44	82.5	79.5	81.5	84.0	81.9
14-46	82.0	81.5	81.0	79.5	81.0
14-48	82.0	81.5	80.5	81.5	81.4
14-49	80.5	82.0	81.5	81.0	81.3

* Tube contained HFIR U₃O₈

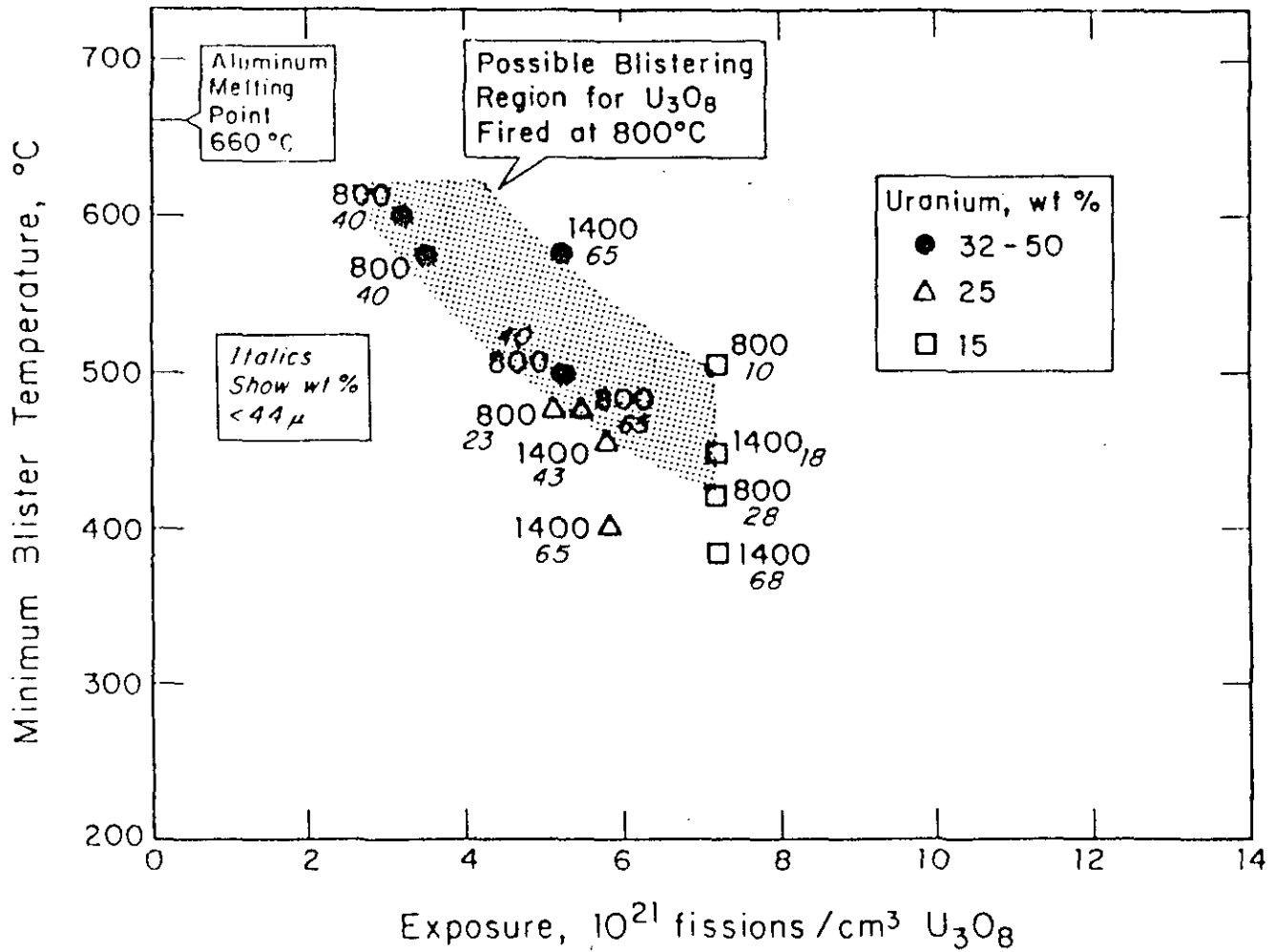
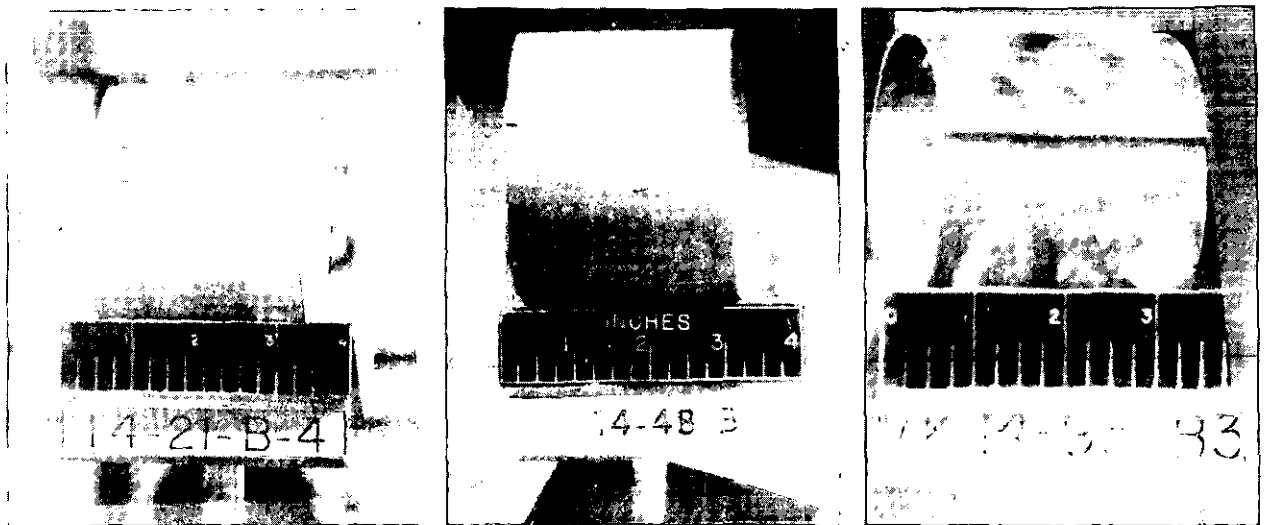


FIGURE 28. BLISTER TEMPERATURE FOR IRRADIATED U₃O₈-ALUMINUM FUEL TUBES

Reference: Peacock, H. B., "Powder Metallurgy at Savannah River Laboratory," E. I. du Pont de Nemours and Company, DP-1524, December 1978

Type 800 U₃O₈



% Uranium	15	25	45
Fiss/cm ³ U ₃ O ₈ (s10 ²⁰)	71	51	35
Min. Blister Temp., °C	425	475	600

FIGURE 29. PHOTOGRAPHS OF BLISTERED U₃O₈-AI SPECIMENS

Metallographic sections showing partially reacted particles from irradiated and blistered tubes are shown in Figure 30. It is expected that the interior contains substoichiometric uranium oxide, and surrounding the particles are aluminum-uranium and aluminum-oxide phases. Porosity exists within the oxide particle and around the particle as well as in the reacted zone. The porosity also appears to be larger in the heated particle than in the as-irradiated particle. After heating, cracks appear within the irradiated oxide particle which tend to follow the porosity. It is expected that cracking results from increase gas pressure within the pores.

5.0 IN-REACTOR FUEL BEHAVIOR

Cermet fuel elements have been irradiated in research and test reactors since the early 60's. The U_3O_8 -aluminum fuel has performed satisfactorily and no known accidents have occurred during irradiation. At SRS 24 elements were irradiated during process development.

5.1 Fuel Element Failures

During development of the PM process at SRS, several fuel failures occurred in the reactor and cooling basin⁽⁵⁰⁾. Failures were not related to irradiation but to fabrication defects or cladding corrosion.

A cladding failure occurred in the reactor from a large agglomerated U_3O_8 particle that thinned the cladding of a 30 wt% U_3O_8 tube. During irradiation, corrosion of the thin area exposed the core.

One of six fuel tubes containing 56 wt% U_3O_8 developed a hole in the cladding while cooling in the basin. No increased moderator activity was detected while in the reactor. Examination after approximately one year in the cooling basin showed a half-inch diameter hole in the cladding near the bottom of the element. Near the vicinity of the hole were other corrosion pits which indicated that the cladding penetration occurred in the basin and that the failure was not associated with irradiation of U_3O_8 fuel. No corrosion of the core material was observed.

5.2 Severe Accident Tests

Studies of metal-water reactions in the Transient Reactor Test Facility (TREAT) were done to determine the physical behavior of typical reactor fuel materials and the extent of their reaction with water under conditions directly simulating a nuclear excursion accident⁽⁵¹⁾. A series of experiments were performed with aluminum- U_3O_8 cermet core fuel elements. Samples were sections from a High Flux Isotope Reactor (HFIR) fuel plate containing 41.45 wt% U_3O_8 .

The experiments consisted of subjecting an autoclave containing the sample which was submerged in 45 cc of water with 60 cc of free volume to a burst of neutrons in TREAT. The extent of the metal-water reaction was calculated from the amount of hydrogen evolved.



a) As-Irradiated 500X



b) Irradiated and Heated 1 Hour at 525°C 1000X

FIGURE 30. U_3O_8 PARTICLES IRRADIATED TO 7.1×10^{21} FISSIONS/CC OF U_3O_8

The results from 12 experiments with HFIR samples indicated the following:

The samples retained their plate-like shape at fission energy inputs as high as 440 cal/g, even though 230 cal/g was sufficient to melt the aluminum.

Samples subjected to energies greater than about 500 cal/g lost their resemblance to plates. In the experiment with an energy input of 645 cal/g, extensive reaction occurred with about 75% of the aluminum reacted. There was only a small number of small aluminum particles present.

The major difference between aluminum-uranium alloys fuels and aluminum-U₃O₈ fuels is the strength which the HFIR material exhibited in retaining its shape at energies higher than that required to completely melt the aluminum.

In conclusion it was postulated that at low energies, where breakup does not occur or the plates do not lose their shape, the aluminum cannot react extensively; the nature of the reaction is to form a protective oxide film and cooling rates are sufficient to prevent ignition. At energies sufficient to cause the plate surface temperatures to reach 1200 to 1400°C (about 530 cal/g), the fuel samples are fluid enough to break up in 30°C water. In 120°C and 285°C water, even though breakup does not occur, the samples are fluid enough to flow and continuously disrupt the protective oxide film. As fresh surface area forms, more extensive reaction occurs. It is likely that energy produced by this surface reaction was sufficient to raise the metal temperature to values where an ignition between aluminum and U₃O₈ can occur. Ignition is followed by nearly complete reaction at an apparent burning temperature of about 2050°C. Although reaction in the burning regime is extensive, the reaction rate is low, requiring about 30 seconds for consumption of an 8mm pellet.

The quantitative similarity between the results of TREAT experiments with aluminum-U₃O₈ cermet fuels and with aluminum-uranium alloy fuels suggested to them that the thermite reaction in the cermet fuel to form Al₂O₃ and aluminum-uranium intermetallic compounds is not an important energy source.

6.0 FISSION PRODUCT RELEASE

Studies were carried out on the release of fission products from irradiated U₃O₈-Al fuel by Woodley⁽⁵²⁾ and were summarized by Whitkop⁽⁵³⁾. These tests were done in air, argon, and steam/argon atmospheres. Temperatures of 850°C and 1000°C were used in the tests.

Fission product release from U₃O₈-Al fuel is different from U-Al fuel. In general, U₃O₈-Al fuel releases less volatile fission products at temperatures less than c.a. 1000°C. At the onset of the exothermic reaction at c.a. 1000°C, the U₃O₈-Al fuel abruptly releases a large portion of the remaining fission products. Noble gases are totally released from oxide fuel when temperatures are greater than 700°C for at least two minutes. Cesium, iodine, and tellurium are released in significant quantities but chemical forms were not identified. Insignificant amounts of Ce, Eu, Ru, and Sb were released from the fuel under any atmosphere and temperature within the range of experimental conditions.

7.0 FABRICABILITY

Billet cores have been isostatically compacted in water at pressures up to 30,000 psi. The cores contained mixtures of U_3O_8 and aluminum powder, and compacts have been made which contain 100% U_3O_8 .

For isostatic compaction, the powder is sealed in an elastomeric bag which prevents it from getting wet. Care must be taken to make sure that no water enters the compact because a slow reaction takes place between aluminum powder and water. Measurements have shown that it takes about 24-48 hours and that the compacted core may reach several hundred degrees centigrade.

During development, over a thousand cermet fuel tubes have been made in SRL by the PM process described in Figure 1. Extrusion studies have been made for billet cores containing up to 80 wt% U_3O_8 in aluminum⁽⁵⁴⁾.

Results of fabrication yield vs wt% oxide is shown in Figure 31. Above approximately 60 wt% U_3O_8 or 50 wt% uranium, the extrusion yield begins to decrease. The acceptable overall fabrication yield for the U-Al plant process has been about 80% and includes other metal working operations such as drawing, roll straightening, machining, and quality control inspection.

With the same extrusion yield criteria as for the U-Al process (80%), the uranium content in cermet fuel can be increased by 43%.

8.0 REPROCESSIBILITY

Studies have been done at SRS on the reprocessing of U_3O_8 -Al fuel tubes. Both unirradiated and irradiated fuel tubes have been processed using the current mercury catalyzed nitric acid dissolution (HM) process in the Canyon at SRS.

8.1 Unirradiated Fuel

The dissolving behavior of unirradiated U_3O_8 -Al fuel tubes is similar to that of U-Al alloy⁽⁵⁶⁾. Tube sections dissolved rapidly in HNO_3 - $Hg(NO_3)_2$ solution, retaining their cylindrical shape even when 89% of the tube was dissolved. This behavior is essentially identical to that of U-Al alloy. The partly dissolved tube is strong and can support the weight of the original tube. The crush strength of partially dissolved sections is shown in Figure 32. Fragments generated by the collapsing tube section, as well as any transient fragments produced, contained a lower concentration of uranium than the original fuel core. This indicated that the uranium oxide in the core dissolves faster than the aluminum in the core. Practically complete dissolution of the test specimens was achieved while insoluble residues amounted to 0.3% or less of the original core. The dissolving rate is shown in Figure 33 (a) for unirradiated cermet fuel tubes in boiling 3M HNO_3 .

Unirradiated tubes containing oxide fired at either 800 or 1400°C have been dissolved in the canyon at SRS.

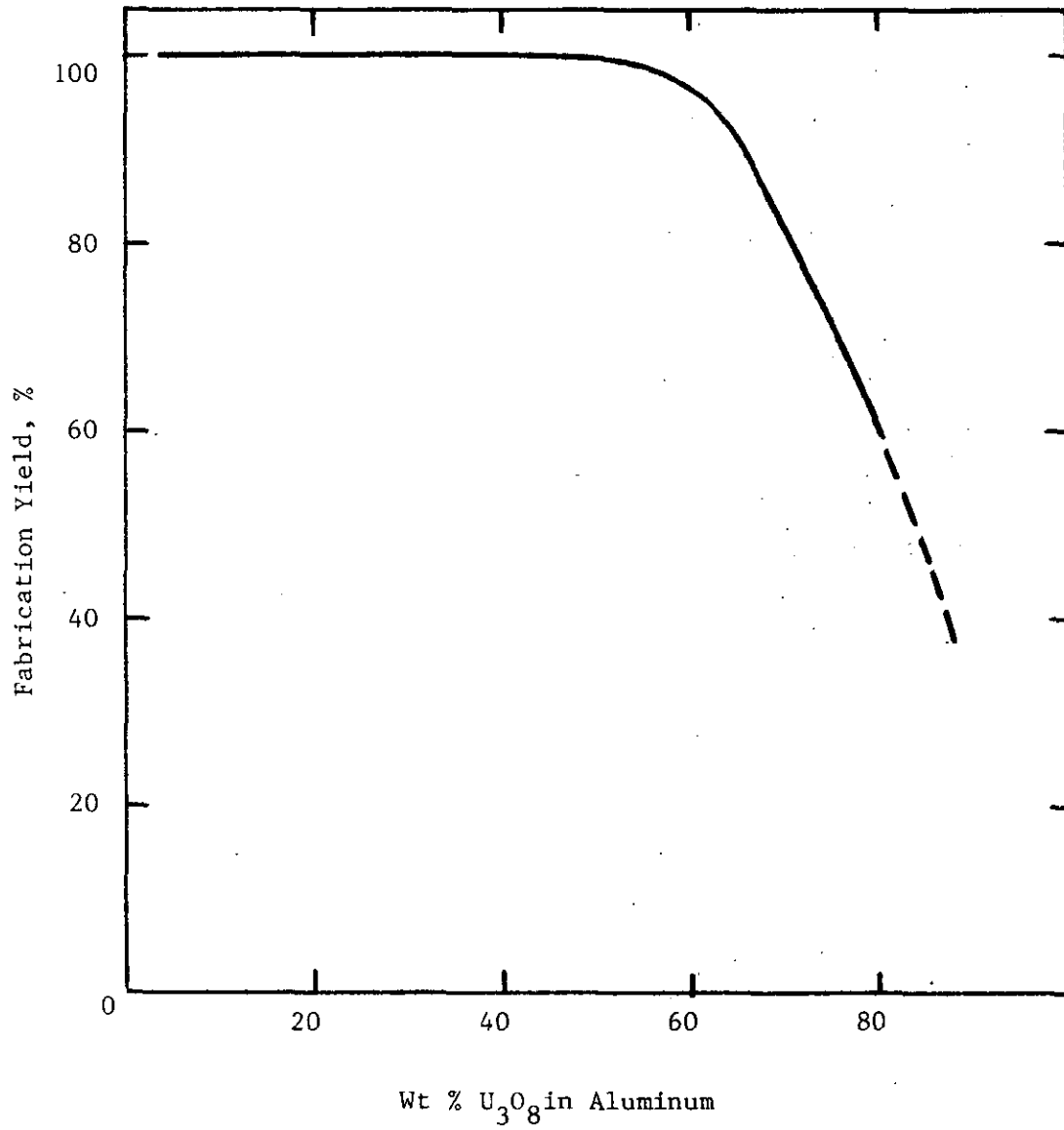


FIGURE 31. EXPECTED FABRICATION YIELD FOR U₃O₈-Al FUEL TUBES, BASED ON DEVELOPMENTAL TESTS

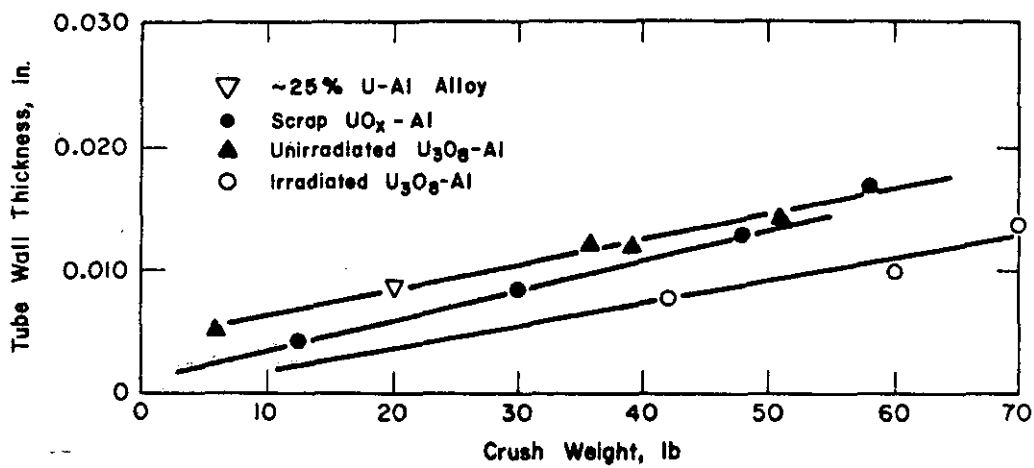
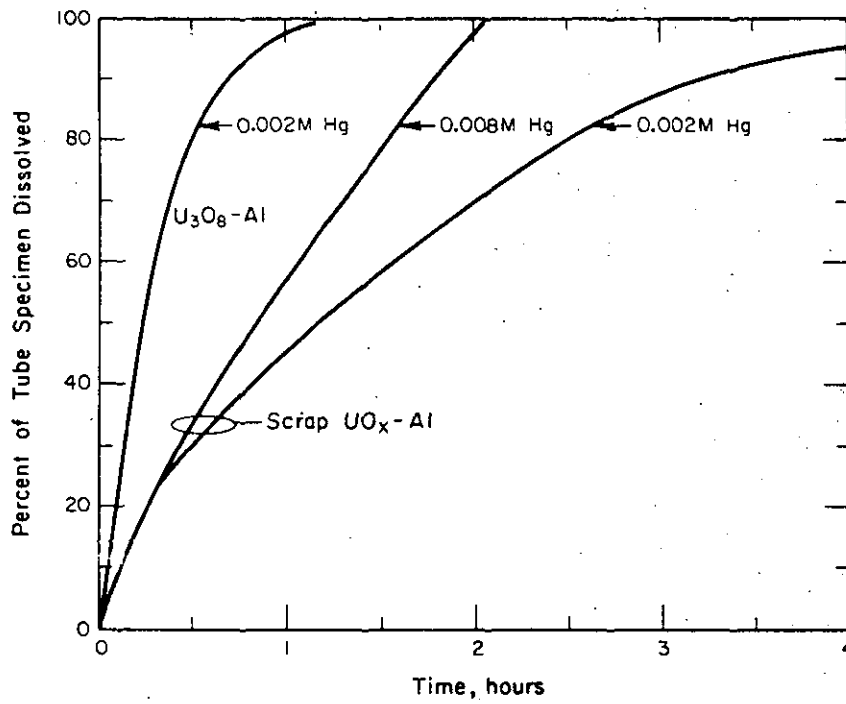
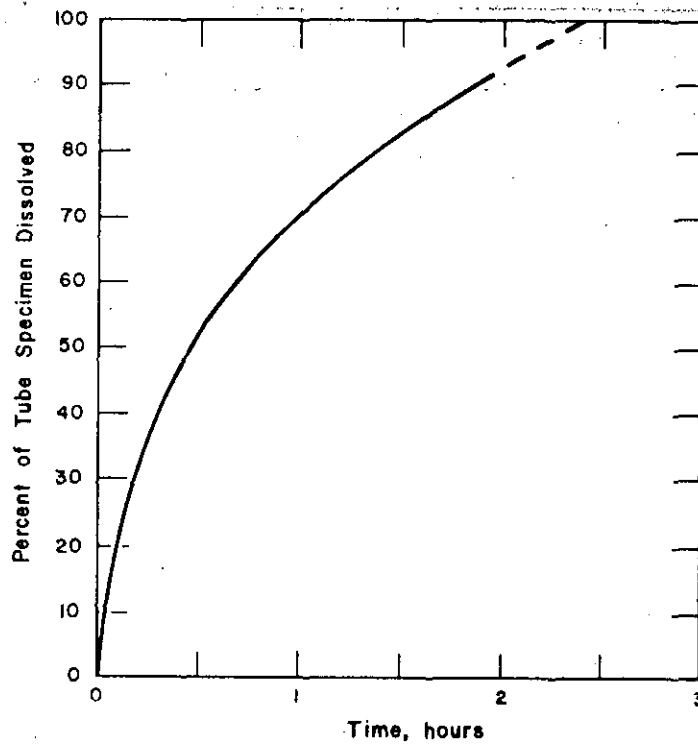


FIGURE 32. STRENGTH OF PARTIALLY DISSOLVED URANIUM OXIDE - AL TUBES (VERTICAL MODE)

Reference: Perkins, W. C., "Dissolving Uranium Oxide-Aluminum Fuel," DP-1337, November 1973



(a) Dissolving Rate of Unirradiated Uranium Oxide-Aluminum Tubes In Boiling 3M HNO₃



(b) Dissolving Rate of Irradiated U₃O₈-Al Tubes In Boiling 3M HNO₃-0.002M Hg(NO₃)₂

FIGURE 33. REPROCESSING OF CERMET FUEL TUBES

Reference: Perkins, W. C., "Dissolving Uranium Oxide-Aluminum Fuel," DP-1337, November 1973

8.2 Irradiated Fuel

Tubes irradiated to about 10^{21} fission/cc require about twice as long to dissolve in 3M HNO₃-0.002M Hg(NO₃)₂ as unirradiated tubes (56, 57). The irradiated cores were also slightly stronger. Otherwise the dissolving behavior was similar.

Irradiated fuel tubes containing up to 65 Wt% U₃O₈ in aluminum have been successfully dissolved at SRS.

9.0 REFERENCES

1. E. S. Bomar, p. 71, "Met. Div. Semiannual Prog. Report for Period Ending April 10, 1953," ORNL-1551.
2. A. E. Richt, C. F. Leitten, Jr., and R. J. Beaver, "Radiation Performance and Induced Transformations in Aluminum-Base Fuels," pp. 469-488 in Research Reactor Fuel Element Conference, September 17-19, 1962, Gatlinburg, TN, TID-7642, Book 2 (1963).
3. J. H. Erwin, R. C. Waugh, and J. H. Coobs, p. 113, "Met. Div. Semiannual Progress Report for Period Ending October 10, 1955," ORNL-1988.
4. R. C. Waugh, p. 139, "Met Div. Annual Progress Report for Period Ending October 10, 1957," ORNL-2422.
5. W. J. Kucera, p. 262, "Met Div. Annual Progress Report for Period Ending September 1, 1959," ORNL-2839.
6. R. J. Beaver and A. E. Richt, p. 95, "Met. Div. Annual Progress Report for Period Ending May 31, 1961," ORNL-3160.
7. G. M. Adamson, Jr., p. 173, "Metals and Ceramics Division Annual Progress Report for Period Ending May 31, 1963," ORNL-3470.
8. W. J. Werner and J. R. Barkman, "Characterization and Production of U_3O_8 for the High Flux Isotope Reactor," ORNL-4052 (April 1967).
9. W. R. Martin, p. 94, "Metals and Ceramics Division Annual Progress Report for Period Ending June 30, 1969," ORNL-4470.
10. R. W. Knight and G. M. Adamson, Jr., p. 214, "Metals and Cermaics Division Annual Progress Report for Period Ending June 30 1965," ORNL-3870.
11. Barkman, S. R., "A Chemical Recovery System for Safeguarding Unirradiated Uranium," Oak Ridge Y-12 Plant, Y-MA-3582, July 1970.
12. Peacock, H. B and Sturken, E.F., "Morphology of Depleted and Enriched Uranium Oxide Powders," E.I. du Pont de Nemours & Co., DPST-75-510, 1975.
13. Szulinske, M. S., "Development of An Agitated Trough Continuous Calciner," Chemical Engineering Progress, Vol. 53, No.12, pp 586-589, 1957.
14. Uranium Solidification Facility, Westinghouse Savannah River Company, Basic Data Report #88-13, 1988.
15. Ackermann, R. S. and Chang, T., "Thermodynamic Characterization of the U_3O_{8-z} Phase," J. Chem. Thermodynamics, Vol. 5, pp 873-890, 1973.
16. Peacock, G. B., "Formation of U_4O_9 in Heated U_3O_8 -Al Powders and compacts," E. I. du Pont de Nemours & Co., DPST-87-729, October 1987.
17. Marra, J. E. and Peacock, G. B., "Reactions During Processing of U_3O_8 -Al Fuels," E. I. du Pont de Nemours & Co., DP-1776, June 1989.

18. Martin, M. M., Werner, W. J. and Leitten, Jr., C. F., "Fabrication of Aluminum-Base Irradiation Test Plates," ORNL-TM-1277, February 1966.
19. Knight, R. W., Binns, J. and Adamson, Jr., G. M., "Fabrication Procedures for Manufacturing High Flux Isotope Reactor Fuel Elements," ORNL-4242, June 1968.
20. Gronvold, Fl, "Crystal Structure of Uranium Oxide (U_3O_8)," Nature 162, pp 69-70, 1948.
21. Handbook of Chemistry and Physics, 36th Edition, Chemical Rubber Publishing Co., 1954-55.
22. Peacock, H. B., "Preparation and Physical Properties of U_3O_8 ," E. I. du Pont de Nemours and Company, DPST-38-276, January 1983.
23. Peacock, H. B., "A Technique to Determine Billet Core Charge Weight for PM Fuel Tubes," E. I. du Pont de Nemours and Company, DPST-84-516, May 1984.
24. Brewer, L., "The Thermodynamic Properties of the Oxides and their Vaporization Processes," Chem. Revs. 52, 1-75, 1953.
25. Martin, M. M., Monthly Report, ORNL-4600, p244, June 1970.
26. Copeland, G. L. and Martin, M. M. "Fabrication of High-Uranium-Loaded U_3O_8 -Al Developmental Fuel Plates," ORNL/TM-7607, December 1980.
27. Jones, W. M., Gordon, J. and Long, A., "The Heat Capacities of Uranium, Uranium Trioxide and Uranium Dioxide from 15°K to 30°K," J. Chem. Phys. 20, 695-699, 1952.
28. Huber, E. J., Holley, C. E. and Mererkard, E. H., "Heats of Combustion of Thorium and Uranium," J. Am. Chem. Soc. 74, 3406-3408, 1952.
29. Coughlin, J. P., "Heats and Free Energy of Formation of Inorganic Oxides," U. S. Bureau of Mines Bull. 542, 1954.
30. Glassner, A., "The Thermochemical Properties of Oxides, Fluorides and Chlorides to 250°K," ANL-5750, 1957.
31. Popov, M. M., Galchenko, G. L. and Senin, M. D., "True Heat Capacities of UO_2 , U_3O_8 and UO_3 at High Temperatures," Zhurnal Neoganecheskoi Khemii, Vol III, No. 8, pp 1734-1737 (J. of Inorganic Chemistry USSR), 1958.
32. Touloukian, Y. S. (dir), "Thermophysical Properties of Matter," Vols 4 and 5.
33. Ross, A. M., "The Dependence of the Thermal Conductivity of Uranium Dioxide on Density, Microstructure, Stoichiometry and Thermal-Neutron Irradiation," Atomic Energy of Canada Limited, AECL-1096 (CRFD-817), 1960.
34. Belle, J., "Properties of Uranium Dioxide," Proceedings of the Second United Nations International Conference of the Peaceful Uses of Atomic Energy, 6, Paper p/2404, 569-589, 1958.

35. Nichols, R. W., "Ceramic Fuels-Properties and Technology," Nuclear Engineering, 3(29), pp 327-233, 1958.
36. Schulz, B., "Anomalie Der Thermischen Ausdehnung Und Wärmeleitfähigkeit Von U_3O_8 ," Rev. int. Htes Temp. et Refract. 12, pp 132-134, 1975.
37. Peacock, H. B., "Thermal Conductivity of U_3O_8 -Al Mixtures," E. I. du Pont de Nemours and Company, DPST-79-349, April 1979.
38. Bruggeman, D.A.G., "Dielectric Constant and Conductivity of Mixtures of Isotropic Materials," Annalen Physic, 24, pp 636-679, 1935.
39. Copeland, G.L. and Martin, M.M., "Fabrication of High Uranium-Loaded U_3O_8 -Al Developmental Fuel Plates," Oak Ridge National Laboratory, ORNL/TM-7606, 1980.
40. Peacock, H. B. and Frontroth, R. L., "Properties of Aluminum-Uranium Alloys," Westinghouse Savannah River Company, WSRC-RR-89-489, August 1989.
41. King, R. T., Long, E. L., Stiegler, J. O. and Farrell, K., "High-Neutron Fluence Damage in an Aluminum Alloy," J. of Nuclear Materials, 35, pp 231-243, 1970.
42. Griffith, W. M., Kim, Y. W. and Froes, F. H., "Powder Metallurgy Processing of Aluminum Alloy 7091," pp 283-303 in Rapidly Solidified Powder Aluminum Alloys, ASTM Special Technical Publication 890, Finke, M. E. and Stark Jr., E. A., eds., American Society for Testing and Materials, Philadelphia, Pennsylvania, 19103, 1986.
43. Fleming, J. D. and Johnson, J. W., "Aluminum- U_3O_8 Exothermic Reactions, Nucleonics, Vol. 2 No. 5, May 1963.
44. Baker, L., Bingle, J. D., Waschal, R. and Barnes, C., "Aluminum U_3O_8 Thermite Reaction," Argonne National Laboratory, ANL 6800, 1964.
45. Peacock, H. B., "Study of the U_3O_8 -Al Thermite Reaction and Strength of Reactor Fuel Tubes," E. I. du Pont de Nemours and Company, DP-1665, August 1983.
46. Pasto, A. E., Copeland, G. L. and Martin, M. M., "Quantitative Differential Thermal Analysis Study of the U_3O_8 -Al Thermite Reaction," Bull of the Am Ceramics Soc., 61, p 491, 1982.
47. Martin, M. M. Richt, A. E. and Martin, W. R., "Irradiation Behavior of Aluminum-Base Fuel Dispersions," Oak Ridge National Laboratory, ORNL-4856, May 1973.
48. Richt, A. E., Knight, R. W. and Adamson, Jr., G. M., "Postirradiation Examination and Evaluation of the Performance of HFIR Fuel Elements," Oak Ridge National Laboratory, ORNL-4714, December 1971.
49. Hofman, G. L., Copeland, G. L. and Sanecki, J. E., "Microscopic Investigation into the Irradiation Behavior of U_3O_8 -Al Dispersion Fuel," Nuclear Technology, Vol 72, pp 338-344, March 1986.
50. Peacock, H. B., "Inspection of Irradiated P-7 Fuel Tubes," E. I. du Pont de Nemours and Company, DPST-80-447, August 20, 1980.

51. Argonne National Laboratory, Chemical Engineering Division Semi-Annual Report, July - December 1965, ANL 7125, May 1966.
52. Woodley, R. E., "The Release of Fission Products From Irradiated SRP Fuels at Elevated Temperature," HEDL-7598, June 1986.
53. Whitkop, P. G., "Summary of the Second Service of SRL Fuel Melt Experiments," E. I. du Pont de Nemours and Company, Savannah River Laboratory, DPST-87-412, July 23, 1987.
54. Peacock, H. B., "Coextrusion of 60 to 30 wt % U_3O_8 Nuclear Fuel Elements, E. I. du Pont de Nemours and Company, DP-MS-80-114, November 1980.
55. Hester, J. R., Raw Materials Works Technical Monthly Report, E. I. du Pont de Nemours and Company, DPSP-79-71-16, 1979.
56. Perkins, W. C., "Dissolving Uranium Oxide-Aluminum Fuel," E. I. du Pont de Nemours and Company, DP-1337, November 1973.
57. Perkins, W. C., "Dissolution of Uranium Oxide - Aluminum Fuel," E. I. du Pont de Nemours and Company, DPST-73-447, September 1973.

ACKNOWLEDGMENTS

The author would like to thank other members of the NPR Fuel Selection Committee for their contributions to this program. In particular we are grateful to G. L. Copeland of Oak Ridge National Laboratory for his help in preparing this report. We also thank Joy McFerrin for preparation and typing of the manuscript.